

Thermodynamics and collapse of self-gravitating Brownian particles in D dimensions

Clément Sire* and Pierre-Henri Chavanis†

Laboratoire de Physique Quantique (UMR 5626 du CNRS), Université Paul Sabatier, 118, route de Narbonne, 31062 Toulouse, France

(Received 17 June 2002; published 24 October 2002)

We address the thermodynamics and the collapse of a self-gravitating gas of Brownian particles in D dimensions, in both canonical and microcanonical ensembles. We study the equilibrium density profile and phase diagram of isothermal spheres and, for $2 < D < 10$, determine the onset of instability in the series of equilibria. We also study the dynamics of self-gravitating Brownian particles in a high friction limit leading to the Smoluchowski-Poisson system. Self-similar solutions describing the collapse are investigated analytically and numerically. In the canonical ensemble (fixed temperature), we derive the analytic form of the density scaling profile which decays as $f(x) \sim x^{-\alpha}$, with $\alpha = 2$. In the microcanonical ensemble (fixed energy), we show that f decays as $f(x) \sim x^{-\alpha_{\max}}$, where α_{\max} is a nontrivial exponent. We derive exact expansions for α_{\max} and f in the limit of large D . Finally, we solve the problem in $D = 2$, which displays rather rich and peculiar features with, in particular, the formation of a Dirac peak in the density profile.

DOI: 10.1103/PhysRevE.66.046133

PACS number(s): 05.90.+m, 64.60.-i, 47.20.-k, 05.70.-a

I. INTRODUCTION

In an earlier paper [1], we studied a model of self-gravitating Brownian particles confined within a three-dimensional spherical box. We considered a high friction limit in which the equations of the problem reduce to the Smoluchowski-Poisson system with appropriate constraints ensuring the conservation of energy (in the microcanonical ensemble) or temperature (in the canonical ensemble) [2]. The equilibrium states (maximum entropy states) correspond to isothermal configurations which are known to exist only above a critical energy or above a critical temperature (see, e.g., Ref. [3]). When no hydrostatic equilibrium exists, we found that the system generates a finite time singularity (i.e., the central density becomes infinite in a finite time) and we derived self-similar solutions describing the collapse. This study was performed both in the microcanonical and canonical ensembles, with emphasis on the inequivalence of ensembles for such a nonextensive system. In the canonical ensemble, we showed that the scaling exponent for the density is $\alpha = 2$ and we determined the invariant profile $f(x)$, satisfying $f(x) \sim x^{-\alpha}$ for $x \rightarrow +\infty$, analytically. In the microcanonical ensemble, the scaling exponent $\alpha \approx 2.21 \dots$ and the corresponding invariant profile $f(x)$ were determined numerically. These values of α are close to those found by other authors [4–7], using different kinetic equations. This agreement may be coincidental but it may also suggest a kind of universality in the collapse regime.

In this paper, we propose to extend our previous analysis to a space of arbitrary dimension D . The interest of this extension is twofold. First, we shall consider an infinite dimension limit $D \rightarrow +\infty$ in which the problem can be solved analytically. In particular, it is possible to determine the scaling exponent $\alpha(D)$ and the profile $f(x, D)$ in the microcanonical ensemble by a systematic expansion procedure in powers of D^{-1} (Sec. III D), while the canonical value is

always $\alpha = 2$ and the profile can be calculated exactly for any dimension (Sec. III C). We show that, already up to order $O(D^{-2})$, the results of the large D expansion agree remarkably well with those found numerically for $D = 3$. Moreover, we show that the nature of the problem changes at two particular dimensions $D = 2$ and $D = 10$. In Sec. II, we compute the equilibrium phase diagram as a function of the dimension. For $2 < D < 10$, the T - E curve has a spiral shape as in three dimensions (3D). For $D > 10$ and $D < 2$, the T - E curve is monotonic. The dimension $D = 2$ is *critical* and requires particular attention that is given in Sec. IV. We show that for $D = 2$ the system generates a Dirac peak (containing a finite fraction of mass) for $T < T_c = GM/4$ in the canonical ensemble while for $D > 2$, the central singularity contains no mass at the collapse time (but a Dirac peak is always formed in the post-collapse regime). The case $D = 2$ has interest in theoretical physics regarding 2D gravity [8] and string theory [9] (in connection with the Liouville field theory). It has also applications in the physics of random surfaces [10] and random potentials [11], 2D turbulence [12] and chemotaxis [13] (for bacterial populations). Finally, the dynamical equations considered in this paper and in Ref. [2] are receiving a growing interest from mathematicians who established rigorous results concerning the existence and unicity of solutions for an arbitrary domain shape without specific symmetry. We refer to the papers of Rosier [14] and Biler and Nadzieja [15], and references therein, for the connection of our study with mathematical results.

II. EQUILIBRIUM STRUCTURE OF ISOTHERMAL SPHERES IN DIMENSION D

A. The maximum entropy principle

Consider a system of particles with mass m interacting via Newtonian gravity in a space of dimension D . The particles are enclosed within a box of radius R so as to prevent evaporation and make a statistical approach rigorous. Let $f(\mathbf{r}, \mathbf{v}, t)$ denote the distribution function of the system, i.e., $f(\mathbf{r}, \mathbf{v}, t) d^D \mathbf{r} d^D \mathbf{v}$ gives the mass of particles whose position

*Email address: Clement.Sire@irsamc.ups-tlse.fr

†Email address: Chavanis@irsamc.ups-tlse.fr

and velocity are in the cell $(\mathbf{r}, \mathbf{v}; \mathbf{r} + d^D \mathbf{r}, \mathbf{v} + d^D \mathbf{v})$ at time t . The integral of f over the velocity determines the spatial density

$$\rho = \int f d^D \mathbf{v}. \quad (1)$$

The total mass of the configuration is

$$M = \int \rho d^D \mathbf{r}. \quad (2)$$

In the mean-field approximation, the total energy of the system can be expressed as

$$E = \frac{1}{2} \int f v^2 d^D \mathbf{r} d^D \mathbf{v} + \frac{1}{2} \int \rho \Phi d^D \mathbf{r} = K + W, \quad (3)$$

where K is the kinetic energy and W the potential energy. The gravitational potential Φ is related to the density by the Newton-Poisson equation

$$\Delta \Phi = S_D G \rho, \quad (4)$$

where S_D is the surface of a unit sphere in a D -dimensional space and G is the constant of gravity. Finally, we introduce the Boltzmann entropy

$$S = - \int f \ln f d^D \mathbf{r} d^D \mathbf{v}, \quad (5)$$

and the free energy (more precisely the Massieu function)

$$J = S - \beta E, \quad (6)$$

where $\beta = 1/T$ is the inverse temperature. If the system is isolated, the equilibrium state maximizes the entropy S at fixed energy E and mass M (microcanonical description). Alternatively, if the system is in contact with a heat bath that maintains its temperature fixed, the equilibrium state maximizes the free energy J at fixed mass M and temperature T (canonical description). It can be shown that for systems interacting via a long-range potential such as gravity, this mean-field description is *exact* in a suitable thermodynamic limit (see Sec. II D).

To solve this variational problem, we shall proceed in two steps. We first maximize S (J) at fixed M , E , (T) and $\rho(\mathbf{r})$. This yields the Maxwell distribution

$$f = \frac{1}{(2\pi T)^{D/2}} \rho(\mathbf{r}) e^{-v^2/2T}. \quad (7)$$

It is now possible to express the energy and the entropy in terms of $\rho(\mathbf{r})$ and T as

$$E = \frac{D}{2} M T + \frac{1}{2} \int \rho \Phi d^D \mathbf{r}, \quad (8)$$

$$S = \frac{D}{2} M \ln T - \int \rho \ln \rho d^D \mathbf{r}, \quad (9)$$

where we have omitted unimportant constant terms in the entropy (9). The entropy and the free energy are now functionals of $\rho(\mathbf{r})$ and we consider their maximization at fixed energy or fixed temperature. Introducing Lagrange multipliers to satisfy the constraints, the critical points of S (at fixed E and M) or J (at fixed T and M) are given by the Boltzmann distribution (see, e.g., Refs. [16,17] for more details),

$$\rho = A e^{-\beta \Phi}. \quad (10)$$

Then, the equilibrium state is obtained by solving the Boltzmann-Poisson equation

$$\Delta \Phi = S_D G A e^{-\beta \Phi}, \quad (11)$$

and relating the Lagrange multipliers to the appropriate constraints. Note that a similar variational problem occurs in the context of two-dimensional turbulence ($D=2$) to characterize large-scale vortices considered as maximum entropy structures [2,18–21]. The analogy between the statistical mechanics of two-dimensional vortices and stellar systems is discussed in Ref. [22].

It is easy to show that there is no global maximum of entropy at fixed mass and energy for $D > 2$ (see Appendix A). We can make the entropy diverge to $+\infty$ by approaching an arbitrarily small fraction of particles in the core ($M_{core} \ll M$) so that the potential energy goes to $-\infty$. Since the total energy is conserved, the temperature must rise to $+\infty$ and this leads to a divergence of the entropy to $+\infty$. Note that if we collapse *all* particles in the core, the entropy would diverge to $-\infty$. Therefore, the formation of a Dirac peak is not thermodynamically favorable in the microcanonical ensemble. For $D=2$, there exists a global entropy maximum for all energies. On the other hand, there is no global maximum of free energy at fixed mass and temperature for $D > 2$ and if $T < T_c = GM/4$ for $D=2$ (see Appendix B). We can make the free energy J diverge to $+\infty$ by collapsing all particles at $r=0$. Therefore, a canonical system is expected to form a Dirac peak. For $D=2$ and $T > T_c$, there exists a global maximum of free energy. For $D < 2$, there exists a global maximum of entropy and free energy for all accessible values of energy and temperature. We refer to Refs. [23,24] for a rigorous proof of these results. When no global maxima of entropy or free energy exist, we can nevertheless look for *local* maxima since they correspond to metastable states that can be relevant for the considered time scales. Of course, the critical points of entropy at fixed E and M are the same as the critical points of free energy at fixed T and M . Only the onset of instability (regarding the second-order variations of S or J with appropriate constraints) will differ from one ensemble to the other. For $D=3$, this stability problem was considered by Antonov [25] and Padmanabhan [16] in the microcanonical ensemble and by Chavanis [17] in the canonical ensemble, by solving an eigenvalue equation connected to the second-order variations of the thermodynamical potential. It was also studied by Lynden-Bell and Wood [26] and Katz [27] by using an extension of Poincaré theory of linear series of equilibria. We shall give the generalization of these results in Sec. II F to the case of a system of arbitrary dimension D .

B. The D -dimensional Emden equation

To determine the structure of isothermal spheres, we introduce the function $\psi = \beta(\Phi - \Phi_0)$, where Φ_0 is the gravitational potential at $r = 0$. Then, the density field can be written as

$$\rho = \rho_0 e^{-\psi}, \tag{12}$$

where ρ_0 is the central density. Introducing the notation $\xi = (S_D G \beta \rho_0)^{1/2} r$ and restricting ourselves to spherically symmetric configurations (which maximize the entropy for a nonrotating system), the Boltzmann-Poisson Eq. (11) reduces to the form

$$\frac{1}{\xi^{D-1}} \frac{d}{d\xi} \left(\xi^{D-1} \frac{d\psi}{d\xi} \right) = e^{-\psi}, \tag{13}$$

which is the D -dimensional generalization of the Emden equation [28]. For $D > 2$, Eq. (13) has a simple explicit solution, the singular sphere

$$e^{-\psi_s} = \frac{2(D-2)}{\xi^2}. \tag{14}$$

The regular solution of Eq. (13) satisfying the boundary conditions

$$\psi = \psi' = 0 \quad \text{at} \quad \xi = 0, \tag{15}$$

must be computed numerically. For $\xi \rightarrow 0$, we can expand the solution in Taylor series and we find that

$$\psi = \frac{1}{2D} \xi^2 - \frac{1}{8D(D+2)} \xi^4 + \frac{1}{24} \frac{D+1}{D^2(D+2)(D+4)} \xi^6 + \dots \tag{16}$$

To obtain the asymptotic behavior of the solutions for $\xi \rightarrow +\infty$, we note that the transformation $t = \ln \xi$, $\psi = 2 \ln \xi - z$ changes Eq. (13) in

$$\frac{d^2 z}{dt^2} + (D-2) \frac{dz}{dt} = -e^z + 2(D-2). \tag{17}$$

For $D > 2$, this corresponds to the damped oscillations of a fictitious particle in a potential $V(z) = e^z - 2(D-2)z$, where z plays the role of position and t the role of time. For $t \rightarrow +\infty$, the particle will come at rest at the bottom of the well at position $z_0 = \ln[2(D-2)]$. Returning to original variables, we find that

$$e^{-\psi} \rightarrow \frac{2(D-2)}{\xi^2} = e^{-\psi_s} \quad \text{for} \quad \xi \rightarrow +\infty. \tag{18}$$

Therefore, the regular solution of the Emden equation (13) behaves like the singular solution for $\xi \rightarrow +\infty$. To determine the next-order correction, we set $z = z_0 + z'$ with $z' \ll 1$. Keeping only terms that are linear in z' , Eq. (17) becomes

$$\frac{d^2 z'}{dt^2} + (D-2) \frac{dz'}{dt} + 2(D-2)z' = 0. \tag{19}$$

The discriminant associated with this equation is $\Delta = (D-2)(D-10)$. It exhibits two critical dimensions $D = 2$ and $D = 10$. For $2 < D < 10$, we have

$$e^{-\psi} = \frac{2(D-2)}{\xi^2} \left\{ 1 + \frac{A}{\xi^{(D-2)/2}} \cos \left(\sqrt{\frac{(D-2)(10-D)}{2}} \xi \right) \times \ln \xi + \delta \right\} \quad (\xi \rightarrow +\infty). \tag{20}$$

The density profile (20) intersects the singular solution (14) infinitely often at points that asymptotically increase geometrically in the ratio $1 : e^{2\pi/\sqrt{(D-2)(10-D)}}$ (see, e.g., Fig. 1 of Ref. [17] for $D = 3$). For $D \geq 10$, we have

$$e^{-\psi} = \frac{2(D-2)}{\xi^2} \left\{ 1 + \frac{1}{\xi^{(D-2)/2}} \left(A \xi^{\sqrt{(D-2)(D-10)}/2} + B \xi^{-\sqrt{(D-2)(D-10)}/2} \right) \right\} \quad (\xi \rightarrow +\infty). \tag{21}$$

For $D = 2$, Eq. (17) can be solved explicitly and we get

$$e^{-\psi} = \frac{1}{\left(1 + \frac{1}{8} \xi^2 \right)^2}. \tag{22}$$

This result has been found by various authors in different fields (see, e.g., Refs. [8,29]). Note that $e^{-\psi} \sim \xi^{-4}$ at large distances instead of the usual ξ^{-2} behavior obtained for $D > 2$. This implies that the mass of an unbounded isothermal sphere is finite in $D = 2$, although it is infinite for $D > 2$.

For $D < 2$, we can neglect e^z on the right-hand side (rhs) of Eq. (17) at large distances and we get

$$e^{-\psi} \sim e^{-A_D \xi^{2-D}} \quad (\xi \rightarrow +\infty), \tag{23}$$

where A_D is a constant depending on the dimension D . For $D = 1$, Eq. (13) can be solved exactly, yielding the result (see, e.g., Ref. [30])

$$e^{-\psi} = \frac{1}{\cosh^2(\xi/\sqrt{2})}, \tag{24}$$

establishing $A_1 = \sqrt{2}$.

C. The Milne variables

As is well known [28], isothermal spheres satisfy a homology theorem: if $\psi(\xi)$ is a solution of the Emden equation, then $\psi(A\xi) - 2 \ln A$ is also a solution, with A an arbitrary constant. This means that the profile of isothermal configurations is always the same (characterized intrinsically

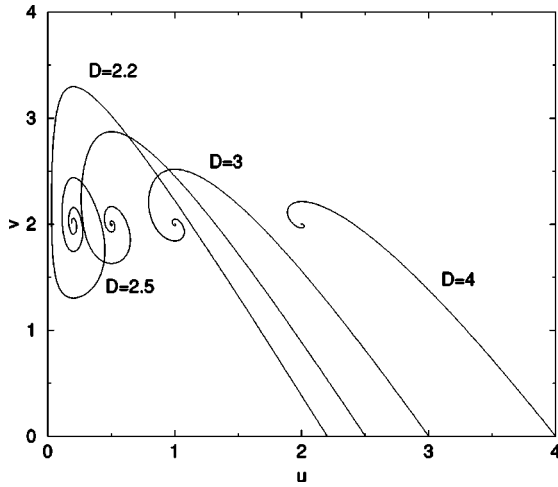


FIG. 1. The solutions of the Emden equation in the (u, v) plane for systems with dimension $2 < D < 10$.

by the function ψ), provided that the central density and the typical radius are rescaled appropriately. Because of this homology theorem, the second-order differential equation (13) can be reduced to a *first-order* differential equation for the Milne variables

$$u = \frac{\xi e^{-\psi}}{\psi'} \quad \text{and} \quad v = \xi \psi'. \quad (25)$$

Taking the logarithmic derivative of u and v with respect to ξ and using Eq. (13), we get

$$\frac{1}{u} \frac{du}{d\xi} = \frac{1}{\xi} (D - v - u), \quad (26)$$

$$\frac{1}{v} \frac{dv}{d\xi} = \frac{1}{\xi} (2 - D + u). \quad (27)$$

Taking the ratio of the foregoing equations, we obtain

$$\frac{u}{v} \frac{dv}{du} = \frac{2 - D + u}{D - u - v}. \quad (28)$$

The solution curve in the (u, v) plane is plotted in Fig. 1 for different values of D . The curve is parametrized by ξ . It starts from the point $(u, v) = (D, 0)$ with a slope $(dv/du)_0 = -(D+2)/D$ corresponding to $\xi=0$. The points of horizontal tangent are determined by $u = D - 2$ and the points of vertical tangent by $u + v = D$. These two lines intersect at $(u_s, v_s) = (D - 2, 2)$, which corresponds to the singular solution (14). For $2 < D < 10$, the solution curve spirals indefinitely around the point (u_s, v_s) . For $D \geq 10$, the curve reaches the point (u_s, v_s) without spiraling. For $D = 2$, we have the explicit solution $v = 2(2 - u)$ so that $(u, v) \rightarrow (0, 4)$ for $\xi \rightarrow +\infty$. For $D < 2$, $(u, v) \rightarrow (0, +\infty)$ for $\xi \rightarrow +\infty$ (see Fig. 2). More precisely,

$$\frac{u e^{v/(2-D)}}{v^{D/(2-D)}} \sim \omega_D \quad (\xi \rightarrow +\infty), \quad (29)$$

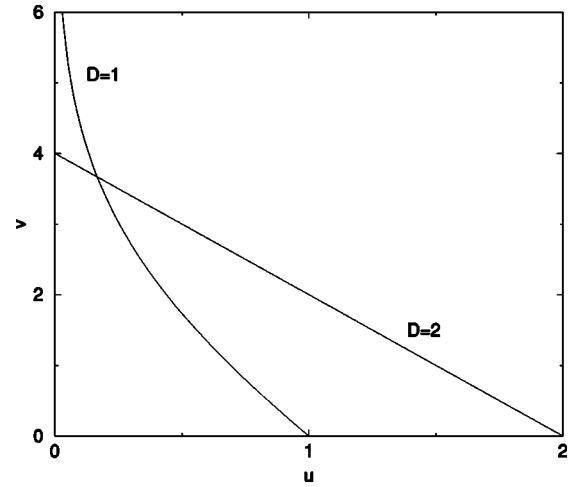


FIG. 2. The solutions of the Emden equation in the (u, v) plane for systems with dimension $D = 1$ and $D = 2$.

where we have defined $\omega_D = 1/[A_D(2-D)^{2(2-D)}]$. For $D = 1$, $\omega_1 = 1/\sqrt{2}$.

D. The thermodynamical parameters

For bounded isothermal systems, the solution of Eq. (13) is terminated by the box at a normalized radius given by $\alpha = (S_D G \beta \rho_0)^{1/2} R$. We shall now relate the parameter α to the temperature and energy. According to the Poisson equation (4), we have for a spherically symmetric distribution of matter,

$$\frac{d\Phi}{dr} = \frac{GM(r)}{r^{D-1}}, \quad (30)$$

where $M(r) \equiv \int_0^r \rho S_D r'^{D-1} dr'$ is the mass within the sphere of radius r (the gravitational field created by a single particle at the origin is $\mathbf{F} = -\nabla\Phi = -Gm/r^{D-1} \mathbf{u}_r$). Equation (30) is the D -dimensional version of the Gauss theorem. Applying this theorem at the box radius, we have

$$GM = \left(r^{D-1} \frac{d\Phi}{dr} \right)_{r=R}. \quad (31)$$

Introducing the dimensionless variables defined previously (using $r/R = \xi/\alpha$), we get

$$\eta \equiv \frac{\beta GM}{R^{D-2}} = \alpha \psi'(\alpha). \quad (32)$$

We note that, for $D = 2$, the parameter η is independent on R . This is a consequence of the logarithmic form of the Newtonian potential in two dimensions.

The computation of the energy is a little more intricate. First, extending the potential tensor theory developed by Chandrasekhar for $D = 3$ (see, e.g., Ref. [31]), we find that the potential energy in D dimensions can be written as

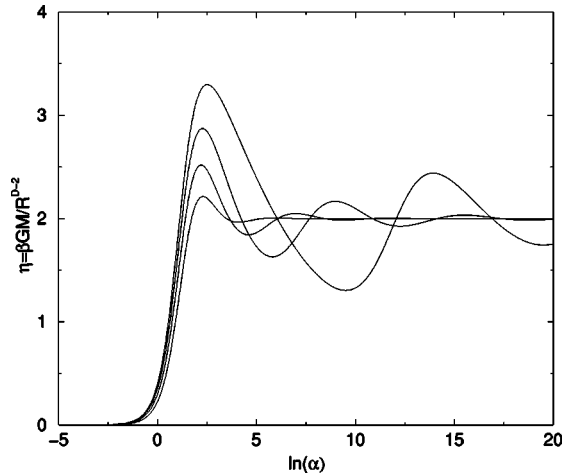


FIG. 3. Evolution of the inverse temperature η along the series of equilibria (parametrized by α) for $2 < D < 10$. The curves correspond to $D=4, 3, 2.5, 2.2$ from bottom to top.

$$W = -\frac{1}{D-2} \int \rho \mathbf{r} \cdot \nabla \Phi d^D \mathbf{r}, \quad (33)$$

for $D \neq 2$. Now, the Boltzmann-Poisson equation (11) is equivalent to the condition of hydrostatic equilibrium

$$\nabla p = -\rho \nabla \Phi, \quad (34)$$

with an equation of state $p = \rho T$. Substituting this relation in Eq. (33) and integrating by parts, we obtain

$$2K + (D-2)W = DV_D R^D p(R), \quad (35)$$

where $V_D = S_D/D$ is the volume of a hypersphere with unit radius. Equation (35) is the form of the Virial theorem in D dimensions. The total energy $E = K + W$ can thus be written

$$E = \frac{D-4}{D-2} K + \frac{D}{D-2} V_D R^D p(R). \quad (36)$$

Expressing the pressure in terms of the Emden function, using $p = \rho T$ and Eq. (12), and using Eq. (32) to eliminate the temperature, we finally obtain

$$\Lambda \equiv -\frac{ER^{D-2}}{GM^2} = \frac{D(4-D)}{2(D-2)} \frac{1}{\alpha \psi'(\alpha)} - \frac{1}{D-2} \frac{e^{-\psi(\alpha)}}{\psi'(\alpha)^2}. \quad (37)$$

It turns out that the normalized temperature and the normalized energy can be expressed very simply in terms of the values of the Milne variables at the normalized box radius. Indeed, writing $u_0 = u(\alpha)$ and $v_0 = v(\alpha)$ and using Eqs. (32) and (37), we get

$$\eta = v_0, \quad (38)$$

$$\Lambda = \frac{1}{v_0} \left[\frac{D(4-D)}{2(D-2)} - \frac{u_0}{D-2} \right]. \quad (39)$$

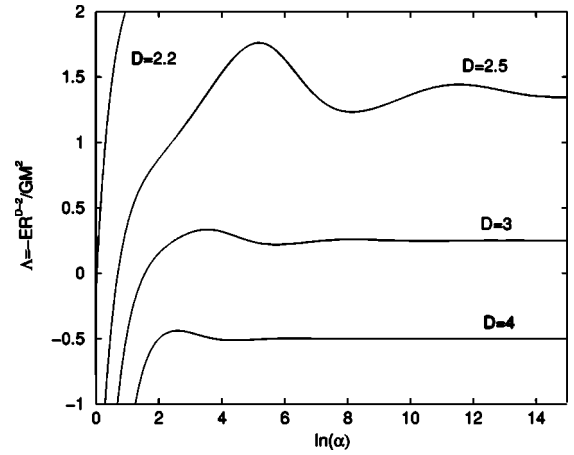


FIG. 4. Evolution of the energy Λ along the series of equilibria (parametrized by α) for $2 < D < 10$.

The curves $\eta(\alpha)$ and $\Lambda(\alpha)$ are plotted in Figs. 3 and 4. For $2 < D < 10$, they exhibit damped oscillations toward the values $\eta_s = 2$ and $\Lambda_s = 1/(D-2) - D/4$, corresponding to the singular solution (14). For $D \geq 10$ the curves are monotonic. For $D = 2$, we have explicitly

$$\eta = \frac{\alpha^2}{2 \left(1 + \frac{1}{8} \alpha^2 \right)},$$

$$\Lambda = \frac{2}{\alpha^2} \left(1 + \frac{\alpha^2}{8} \right) \left\{ \frac{8}{\alpha^2} \left(1 + \frac{\alpha^2}{8} \right) \ln \left(1 + \frac{\alpha^2}{8} \right) - 2 \right\}. \quad (40)$$

The expression of the energy has been obtained directly from Eq. (8) with the boundary condition $\Phi(R) = 0$. The inverse temperature increases monotonically with α up to the asymptotic value $\eta_c = 4$. Using Eq. (22) and returning to the original variables, we can write the density profile in the form

$$\rho = \frac{4M}{\pi R^2 (4 - \eta) \left(1 + \frac{\eta}{4 - \eta} \frac{r^2}{R^2} \right)^2}. \quad (41)$$

This density profile is represented in Fig. 5 for different temperatures. At the critical inverse temperature $\eta_c = 4$, all the particles are concentrated at the center of the domain. The density profile approaches the Dirac distribution

$$\rho(\mathbf{r}) \rightarrow M \delta(\mathbf{r}) \quad \text{for } \eta \rightarrow \eta_c = 4, \quad (42)$$

which has an infinite (negative) energy.

For $D < 2$, the curves $\eta(\alpha)$ and $\Lambda(\alpha)$ are monotonic and tend to $+\infty$ and 0, respectively, as $\alpha \rightarrow +\infty$. For $D = 1$, we have explicitly

$$\eta = \sqrt{2} \alpha \tanh(\alpha/\sqrt{2}), \quad \Lambda = -\frac{3}{2\sqrt{2}} \frac{1}{\alpha \tanh(\alpha/\sqrt{2})} + \frac{1}{2 \sinh^2(\alpha/\sqrt{2})}. \quad (43)$$

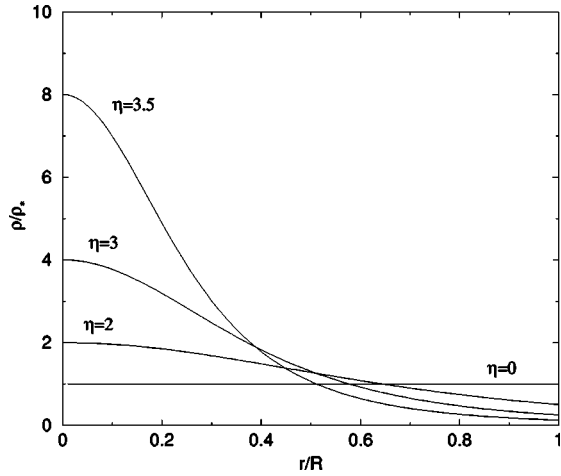


FIG. 5. Equilibrium density profile of a two-dimensional self-gravitating system as a function of the inverse temperature η . For $\eta=0$, the density is uniform. For $\eta \rightarrow \eta_c=4$, the density tends to a Dirac peak. For $\eta > \eta_c$, there is no equilibrium state.

Note that according to Eq. (33), the potential energy is necessarily positive for $D < 2$, so the region $\Lambda \geq 0$ is forbidden. Returning to original variables, the density profile is given by

$$\rho = \frac{M}{2\sqrt{2}R} \frac{\alpha}{\tanh(\alpha/\sqrt{2})} \frac{1}{\cosh^2\left(\frac{\alpha r}{\sqrt{2}R}\right)}, \quad (44)$$

where we recall that $S_1=2$. For $\alpha \rightarrow +\infty$, the profile tends to a Dirac peak $M\delta(\mathbf{r})$.

In Figs. 6 and 7, we have plotted the equilibrium phase diagram $\Lambda-\eta$, giving the temperature as a function of the energy, for different dimensions D . For $2 < D < 10$, the curve spirals around the limit point (Λ_s, η_s) corresponding to the singular solution. For $D \geq 10$, the curve is monotonic until the limit point. For $D=2$, the curve is explicitly given by

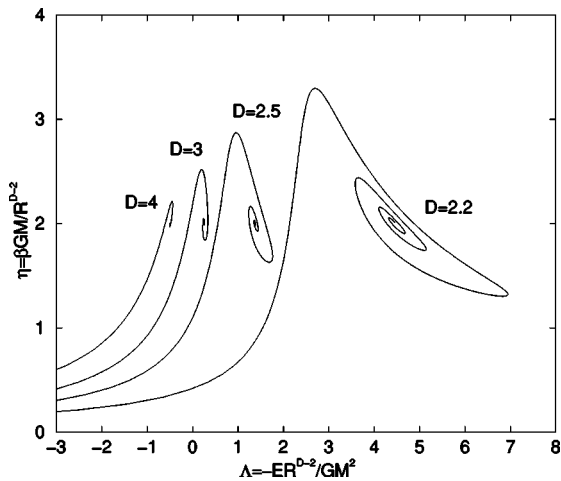


FIG. 6. Equilibrium phase diagram giving the inverse temperature η as a function of the negative of the energy Λ for systems with dimension $2 < D < 10$.

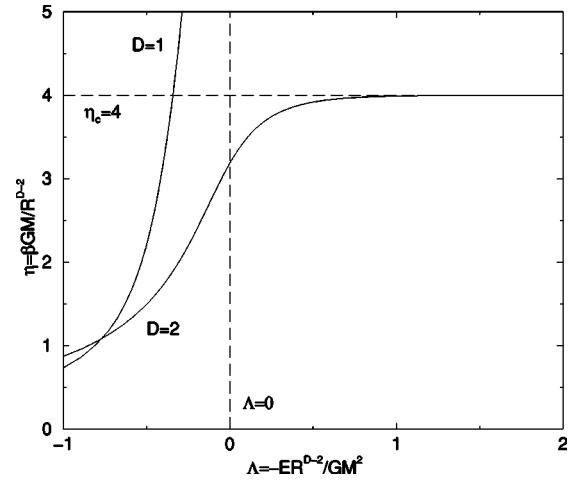


FIG. 7. Equilibrium phase diagram for two-dimensional self-gravitating systems. For infinitely negative energies, the inverse temperature tends to the value $\eta_c=4$. We have also represented the caloric curve for $D=1$.

$$\Lambda = \frac{1}{\eta} \left[\frac{4}{\eta} \ln\left(\frac{4}{4-\eta}\right) - 2 \right], \quad (45)$$

and is represented in Fig. 7, together with the case $D=1$.

We stress that the preceding results, obtained in the mean-field approximation, are exact in the thermodynamic limit $N \rightarrow +\infty$ such that η and Λ are kept fixed. If the box radius is given, this implies that $T \sim N$ and $E \sim N^2$. Alternatively, if the temperature and the energy per particle are given, the thermodynamic limit is such that $N \rightarrow +\infty$ with N/R^{D-2} constant (for $D > 2$).

E. The minimum temperature and minimum energy

For $2 < D < 10$, the curve $\eta(\alpha)$ presents an extremum at points α_n such that $d\eta/d\alpha(\alpha_n)=0$. Using Eqs. (38) and (27), we find that this condition is equivalent to

$$u_0 = D - 2 = u_s. \quad (46)$$

Since the curve $u = u_s$ passes through the center of the spiral in the (u, v) plane, this determines an infinity of solutions (see Fig. 8), one at each extremum of v (since $\eta = v_0$). Asymptotically, the α_n follow a geometric progression (see Ref. [17] for more details):

$$\alpha_n \sim e^{2\pi n / \sqrt{(D-2)(10-D)}} \quad (n \rightarrow +\infty, \text{ integer}). \quad (47)$$

In Fig. 3, we see that an equilibrium state exists only for

$$\eta = \frac{\beta GM}{R^{D-2}} \leq \eta(\alpha_1), \quad (2 < D < 10). \quad (48)$$

This determines a maximum mass (for given T and R) or a minimum temperature (for given M and R) beyond which no equilibrium state is possible. In that case, the system is expected to undergo an *isothermal collapse* (see Sec. III C). For $D=2$ and for $D \geq 10$, the $\eta(\alpha)$ curve is monotonic. An equilibrium state exists provided that

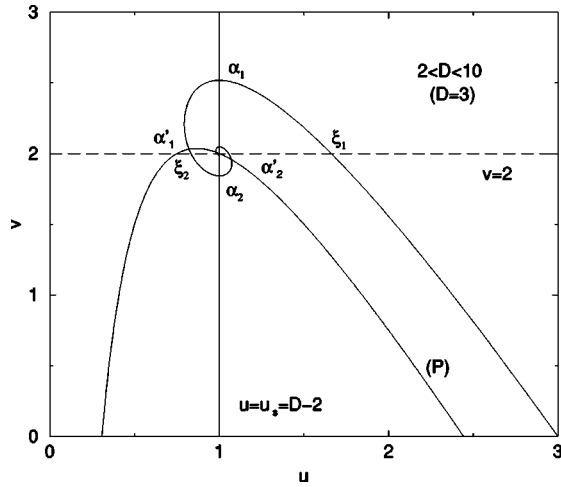


FIG. 8. Location of the turning points of energy and temperature in the (u, v) plane for systems with dimension $2 < D < 10$. The construction is made explicitly for $D=3$, which corresponds to the case extensively studied in Refs. [16,17]. The dashed line $v=2$ determines the location of the nodes of the density profiles that trigger the instabilities in the canonical ensemble (see Sec. II F).

$$\eta = \beta GM \leq \eta_c = 4 \quad (D=2), \quad (49)$$

$$\eta = \frac{\beta GM}{R^{D-2}} \leq \eta_s = 2 \quad (D \geq 10). \quad (50)$$

We get comparable results for the energy. For $2 < D < 10$, the curve $\Lambda(\alpha)$ presents an extremum at points α'_n such that $d\Lambda/d\alpha(\alpha'_n) = 0$. Using Eqs. (39), (26), and (27), we find that this condition is equivalent to

$$4u_0^2 + 2u_0v_0 + (D^2 - 8D + 4)u_0 + D(D-2)(4-D) = 0. \quad (51)$$

We can check that the limit point (u_s, v_s) is a solution of this equation. Therefore, the intersection of the parabola (P) defined by Eq. (51) with the spiral in the (u, v) plane determines an infinity of points α'_n at which the energy is extremum (see Fig. 8). In Fig. 4, we see that an equilibrium state exists only for

$$\Lambda = \frac{-ER^{D-2}}{GM^2} \leq \Lambda(\alpha'_1) \quad (2 < D < 10). \quad (52)$$

This determines a minimum energy (for given M and R) or a maximum radius (for given M and E) beyond which no equilibrium state exists. In that case, the system is expected to collapse and overheat; this is called *gravothermal catastrophe* (see Sec. III D). For $D \geq 10$, the curve $\Lambda(\alpha)$ is monotonic. An equilibrium state exist only for

$$\Lambda = \frac{-ER^{D-2}}{GM^2} \leq \Lambda_s = \frac{1}{D-2} - \frac{D}{4} \quad (D \geq 10). \quad (53)$$

For $D=2$, there exists an equilibrium state for each value of energy (see Fig. 7): there is no gravothermal catastrophe in the microcanonical ensemble in two dimensions [8]. For D

< 2 , there exists an equilibrium state for all accessible values of energy ($\Lambda < 0$) and temperature ($\eta > 0$) (see also Ref. [32] for $D=1$).

F. The thermodynamical stability

We now study the thermodynamical stability of self-gravitating systems in various dimensions. We start by the canonical ensemble which is simpler in a first approach. A critical point of free energy at fixed mass and temperature is a local *maximum* if, and only if, the second-order variations

$$\delta^2 J = - \int \frac{(\delta\rho)^2}{2\rho} d^D \mathbf{r} - \frac{1}{2T} \int \delta\rho \delta\Phi d^D \mathbf{r} \quad (54)$$

are negative for any perturbation $\delta\rho$ that conserves mass, i.e.,

$$\int \delta\rho d^D \mathbf{r} = 0. \quad (55)$$

This is the condition of thermodynamical stability in the canonical ensemble. Introducing the function $q(r)$ by the relation

$$\delta\rho = \frac{1}{S_D r^{D-1}} \frac{dq}{dr}, \quad (56)$$

and following a procedure similar to the one adopted in Ref. [17], we can put the second order variations of free energy in the quadratic form

$$\delta^2 J = \frac{1}{2} \int_0^R dr q \left[\frac{G}{Tr^{D-1}} + \frac{d}{dr} \left(\frac{1}{S_D \rho r^{D-1}} \frac{d}{dr} \right) \right] q. \quad (57)$$

The second-order variations of free energy can be positive (implying instability) only if the differential operator that occurs in the integral has positive eigenvalues. We need, therefore, to consider the eigenvalue problem

$$\left[\frac{d}{dr} \left(\frac{1}{S_D \rho r^{D-1}} \frac{d}{dr} \right) + \frac{G}{Tr^{D-1}} \right] q_\lambda(r) = \lambda q_\lambda(r), \quad (58)$$

with $q_\lambda(0) = q_\lambda(R) = 0$ in order to satisfy the conservation of mass. If all the eigenvalues λ are negative, then the critical point is a maximum of free energy. If at least one eigenvalue is positive, the critical point is an unstable saddle point. The point of marginal stability, i.e., the value of α in the series of equilibria $\eta(\alpha)$ at which the solutions pass from local maxima of free energy to unstable saddle points, is determined by the condition that the largest eigenvalue is equal to zero ($\lambda = 0$). We thus have to solve the differential equation

$$\frac{d}{dr} \left(\frac{1}{S_D \rho r^{D-1}} \frac{dF}{dr} \right) + \frac{GF}{Tr^{D-1}} = 0 \quad (59)$$

with $F(0) = F(R) = 0$. Introducing the dimensionless variables defined previously, we can rewrite this equation in the form

$$\frac{d}{d\xi} \left(\frac{e^\psi}{\xi^{D-1}} \frac{dF}{d\xi} \right) + \frac{F(\xi)}{\xi^{D-1}} = 0 \quad (60)$$

with $F(0) = F(\alpha) = 0$. If

$$\mathcal{L} \equiv \frac{d}{d\xi} \left(\frac{e^\psi}{\xi^{D-1}} \frac{d}{d\xi} \right) + \frac{1}{\xi^{D-1}} \quad (61)$$

denotes the differential operator that occurs in Eq. (60), we can check by using the Emden equation (13) that

$$\mathcal{L}(\xi^{D-1}\psi') = \psi', \quad \mathcal{L}(\xi^D e^{-\psi}) = (D-2)\psi'. \quad (62)$$

Therefore, the general solution of Eq. (60) satisfying the boundary conditions at $\xi=0$ is

$$F(\xi) = c_1(\xi^D e^{-\psi} - (D-2)\xi^{D-1}\psi'). \quad (63)$$

Using Eq. (63) and introducing the Milne variables (25), the condition $F(\alpha) = 0$ can be written

$$u_0 = D - 2. \quad (64)$$

This relation determines the points at which a new eigenvalue becomes positive ($\lambda = 0^+$). Comparing with Eq. (46), we see that a mode of stability is lost each time that η is extremum in the series of equilibria, in agreement with the turning point criterion of Katz [27] in the canonical ensemble. In particular, the series of equilibria becomes unstable at the point of minimum temperature (or maximum mass) α_1 . This corresponds to the point of infinite specific heat $C = dE/dT \rightarrow \infty$, just before entering the region $C < 0$ (see Fig. 6). This is, of course, satisfactory on a physical point of view since negative specific heats are forbidden in the canonical ensemble. Secondary modes of instability appear at values $\alpha_2, \alpha_3, \dots$. We obtain the same results by considering the dynamical stability of isothermal gaseous spheres with respect to the Navier-Stokes equations (see Ref. [17] for $D=3$). Therefore, dynamical and thermodynamical stability criteria coincide for isothermal gaseous spheres.

According to Eq. (56), the perturbation profile that triggers a mode of instability at the critical point $\lambda=0$ is given by

$$\frac{\delta\rho}{\rho_0} = \frac{1}{S_D \xi^{D-1}} \frac{dF}{d\xi}, \quad (65)$$

where $F(\xi)$ is given by Eq. (63). Introducing the Milne variables (25), we get

$$\frac{\delta\rho}{\rho} = \frac{c_1}{S_D} (2-v). \quad (66)$$

The density perturbation $\delta\rho$ becomes zero at point(s) ξ_i such that $v(\xi_i) = 2$. The number of zeros is therefore given by the number of intersections between the spiral in the (u, v) plane and the line $v = 2$ (see Fig. 8). For the n th mode of instability we need to follow the spiral up to the n th extremum of v (since α_n corresponds to an extremum of η , hence v).

Therefore, the density perturbation $\delta\rho$ corresponding to the n th mode of instability has n zeros $\xi_1, \xi_2, \dots, \xi_n < \alpha_n$. Asymptotically, the zeros follow a geometric progression with ratio $e^{2\pi/\sqrt{(D-2)(10-D)}}$ [17]. Note also that the first mode of instability has only one node.

In the microcanonical ensemble, the condition of thermodynamical stability requires that the equilibrium state is an entropy maximum at fixed mass and energy. This condition can be written as

$$\delta^2 S = - \int \frac{(\delta\rho)^2}{2\rho} d^D \mathbf{r} - \frac{1}{2T} \int \delta\rho \delta\Phi d^D \mathbf{r} - \frac{1}{DMT^2} \left(\int \Phi \delta\rho d^D \mathbf{r} \right)^2 < 0, \quad (67)$$

for any variation $\delta\rho$ that conserves mass [the conservation of energy has already been taken into account in obtaining Eq. (67)]. Now, following a procedure similar to that of Ref. [16] in $D=3$, the second variations of entropy can be put in a quadratic form

$$\delta^2 S = \int_0^R \int_0^R dr dr' q(r) K(r, r') q(r'), \quad (68)$$

with

$$K(r, r') = - \frac{1}{DMT^2} \frac{d\Phi}{dr}(r) \frac{d\Phi}{dr}(r') + \frac{1}{2} \delta(r-r') \left[\frac{G}{Tr^{D-1}} + \frac{d}{dr} \left(\frac{1}{S_D \rho r^{D-1}} \frac{d}{dr} \right) \right]. \quad (69)$$

The problem of stability can therefore be reduced to the study of the eigenvalue equation

$$\int_0^R dr' K(r, r') F_\lambda(r') = \lambda F_\lambda(r), \quad (70)$$

with $F_\lambda(0) = F_\lambda(R) = 0$. The point of marginal stability ($\lambda = 0$) will be determined by solving the differential equation

$$\frac{d}{dr} \left(\frac{1}{S_D \rho r^{D-1}} \frac{dF}{dr} \right) + \frac{GF}{Tr^{D-1}} = \frac{2V}{DMT^2} \frac{d\Phi}{dr}(r), \quad (71)$$

with

$$V = \int_0^R \frac{d\Phi}{dr}(r') F(r') dr'. \quad (72)$$

Introducing the dimensionless variables defined previously, this is equivalent to

$$\frac{d}{d\xi} \left(\frac{e^\psi}{\xi^{D-1}} \frac{dF}{d\xi} \right) + \frac{F}{\xi^{D-1}} = \chi \frac{d\psi}{d\xi}, \quad (73)$$

with

$$\chi = \frac{2}{D\alpha^{D-1}\psi'(\alpha)} \int_0^\alpha \frac{d\psi}{d\xi}(\xi') F(\xi') d\xi', \quad (74)$$

and $F(0) = F(\alpha) = 0$. Using the identities (62), we can check that the general solution of Eq. (73) satisfying the boundary conditions for $\xi=0$ and $\xi=\alpha$ is

$$F(\xi) = \frac{\chi}{D-2-u_0} [\xi^D e^{-\psi} - (D-2)\xi^{D-1}\psi'] + \chi\xi^{D-1}\psi'. \quad (75)$$

The point of marginal stability is then obtained by substituting the solution (75) in Eq. (74). Using the identities

$$\int_0^\alpha \psi' \xi^D e^{-\psi} d\xi = \alpha^{D-1}\psi'(\alpha)(D-u_0), \quad (76)$$

$$(D-2) \int_0^\alpha \xi^{D-1}(\psi')^2 d\xi = \alpha^{D-1}\psi'(\alpha)(2D-2u_0-v_0), \quad (77)$$

which result from simple integrations by parts and from the properties of the Emden equation (13) (see Appendix C), it is found that the point of marginal stability is determined by the condition (51). Therefore, the series of equilibria becomes unstable at the point of minimum energy in agreement with the turning point criterion of Katz [27] in the microcanonical ensemble. Note that negative specific heats $C < 0$ are allowed in the microcanonical ensemble until $C = 0$ (i.e., the corresponding isothermal spheres are stable).

According to Eqs. (65) and (75), the perturbation profile that triggers a mode of instability at the critical point $\lambda = 0$ is given by

$$\frac{\delta\rho}{\rho} = \frac{\chi}{S_D} \frac{1}{D-2-u_0} (D-v-u_0), \quad (78)$$

where we have used the Emden equation (13) and introduced the Milne variables (25). The number of nodes in the perturbation profile can be determined with the graphical construction described in Ref. [16] for $D=3$. For $2 < D < 3.32$, it is found that the first mode of instability has a core-halo structure (i.e., two nodes) in continuity with the case $D=3$, while for $3.32 < D < 10$ the perturbation profile has only one node (see Fig. 9).

We can note that the structure of the perturbation profiles triggering the gravitational instability at the critical points (in microcanonical and canonical ensembles) qualitatively agrees with the structure of the density profiles that we have constructed in Appendixes A and B to show the absence of global maximum of entropy or free energy. In the microcanonical ensemble, we showed that for $D < 4$, the system has to break into a ‘‘core’’ and a ‘‘halo’’ in order to increase entropy by a large amount while this separation is not necessary for $D > 4$. Analogously, the perturbation profile (78) has a ‘‘core-halo’’ structure for $D < 3.32$ and not for $D > 3.32$. On the other hand, in the canonical ensemble, we indicate in Appendix B that the natural tendency of the system is to form a Dirac peak instead of a core-halo structure.

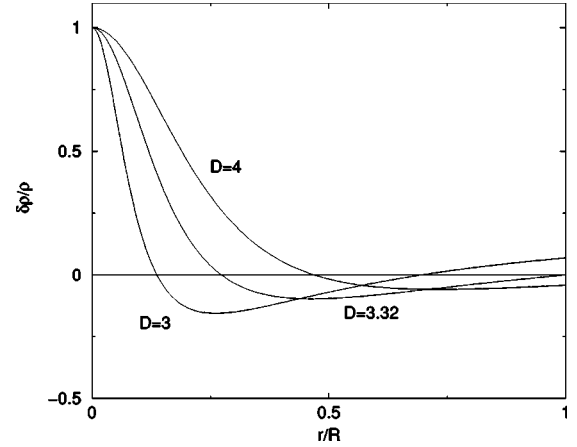


FIG. 9. Perturbation profile corresponding to the first mode of instability in the microcanonical ensemble for various dimensions of space. The profile has two nodes for $D \leq 3.32$ (core-halo structure) and only one node for $D > 3.32$.

This is in agreement with the perturbation profile (66) of the first mode of instability in the canonical ensemble which has *no* core-halo profile [17].

The thermodynamical stability analysis presented in this section also shows that the equilibrium states for $D \leq 2$ and $D \geq 10$ are always stable since the series of equilibria do not present turning points of energy or temperature. Note finally that the grand canonical, grand microcanonical, and isobaric ensembles have been considered in Ref. [33] for $D=3$; these results can be easily extended to a space of arbitrary dimension D with only minor modifications.

III. DYNAMICS OF SELF-GRAVITATING BROWNIAN PARTICLES IN DIMENSION D

A. The Smoluchowski-Poisson system

We now consider the dynamics of a system of self-gravitating Brownian particles in a space of dimension D . As in Ref. [1], we consider a high friction limit in order to simplify the problem. We thus study the Smoluchowski equation [34]

$$\frac{\partial\rho}{\partial t} = \nabla \cdot \left[\frac{1}{\xi} (T\nabla\rho + \rho\nabla\Phi) \right], \quad (79)$$

coupled to the Newton-Poisson equation (4). In the microcanonical ensemble, the temperature $T(t)$ evolves in time so as to satisfy the energy constraint (8). In the canonical ensemble, the temperature T is constant. The Smoluchowski equation can be obtained from a variational principle called the maximum entropy production principle [2]. This variational approach is interesting as it makes a direct link between the dynamics and the thermodynamics. In the microcanonical description, the rate of entropy production can be put in the form (see Ref. [2] and Appendix D)

$$\dot{S} = \int \frac{1}{T\rho\xi} (T\nabla\rho + \rho\nabla\Phi)^2 d^D\mathbf{r} \geq 0, \quad (80)$$

which follows immediately from Eqs. (8), (9), and (79). For a stationary solution, $\dot{S}=0$ and we obtain the Boltzmann distribution (10) which is a critical point of entropy. Considering a small perturbation around equilibrium, we can establish the identity [1]

$$\delta^2 \dot{S} = 2\lambda \delta^2 S \geq 0, \quad (81)$$

where λ is the growth rate of the perturbation defined such that $\delta\rho \sim e^{\lambda t}$. This relation shows that a stationary solution of the Smoluchowski-Poisson system is dynamically stable against small perturbations if and only if it is a local entropy maximum. In addition, the eigenvalue problem determining the growth rate λ of the perturbation is similar to the eigenvalue problem (70) associated with the second-order variations of entropy (they coincide for marginal stability) [1]. This shows the equivalence between dynamical and thermodynamical stabilities for self-gravitating Brownian particles. We get similar results in the canonical ensemble with J in place of S . The relation (81) has been found for other kinetic equations satisfying a H theorem [35]. Finally, we note that the Smoluchowski-Poisson system satisfies a Virial theorem of the form (Appendix D)

$$\frac{1}{2} \xi \frac{dI}{dt} = 2K + (D-2)W - Dp_b V, \quad (82)$$

where

$$I = \int \rho r^2 d^D \mathbf{r} \quad (83)$$

is the moment of inertia and p_b is the pressure on the box (assumed uniform). In the following, we determine self-similar solutions of the Smoluchowski-Poisson system describing the collapse regime. For $E > E_c$ (in the microcanonical ensemble) or $T > T_c$ (in the canonical ensemble), the solutions of the Smoluchowski-Poisson system can either relax towards the local entropy (or free energy) maximum (see Sec. II) or collapse. The choice between these two behaviors depends on a complicated notion of basin of attraction as sketched in Ref. [1] in $D=3$. Unlike the ordinary Smoluchowski equation (without self-gravity) the stationary solution of the Smoluchowski-Poisson system (when it exists) does not attract all dynamical solutions since it is only a *local* maximum of the thermodynamical potential for $D > 2$. Other evolutions (collapse) are possible and lead to larger values of entropy or free energy.

The Smoluchowski-Poisson system can be viewed as a prototype of kinetic equations for self-gravitating systems and is much simpler than the more realistic Landau or Fokker-Planck equations. Possible astrophysical applications regarding planetesimal formation in the solar nebula or violent relaxation of collisionless stellar systems are evoked in Ref. [1]. The Smoluchowski-Poisson system can also describe the relaxation of a gas of point vortices in two dimensions towards a self-organized state (macrovortex). In that context, it can be deduced from the N -body Liouville equation of the point vortex gas by using projection operator

methods [36]. Finally, the Smoluchowski-Poisson system provides a simple model to describe the process of chemotaxis for bacterial populations [13].

B. Self-similar solutions of the Smoluchowski-Poisson system

From now on, we set $M=R=G=\xi=1$. The equations of the problem become

$$\frac{\partial \rho}{\partial t} = \nabla \cdot (T \nabla \rho + \rho \nabla \Phi), \quad (84)$$

$$\Delta \Phi = S_D \rho, \quad (85)$$

$$E = \frac{D}{2} T + \frac{1}{2} \int \rho \Phi d^D \mathbf{r}, \quad (86)$$

with boundary conditions

$$\frac{\partial \Phi}{\partial r}(0, t) = 0, \quad \Phi(1) = \frac{1}{2-D}, \quad T \frac{\partial \rho}{\partial r}(1) + \rho(1) = 0, \quad (87)$$

for $D > 2$. For $D=2$, we take $\Phi(1)=0$ on the boundary. We restrict ourselves to spherically symmetric solutions. Integrating Eq. (85) once, we can rewrite the Smoluchowski-Poisson system in the form of a single integrodifferential equation

$$\frac{\partial \rho}{\partial t} = \frac{1}{r^{D-1}} \frac{\partial}{\partial r} \left\{ r^{D-1} \left(T \frac{\partial \rho}{\partial r} + \frac{\rho}{r^{D-1}} \int_0^r \rho(r') S_D r'^{D-1} dr' \right) \right\}. \quad (88)$$

The Smoluchowski-Poisson system is also equivalent to a single differential equation

$$\frac{\partial M}{\partial t} = T \left(\frac{\partial^2 M}{\partial r^2} - \frac{D-1}{r} \frac{\partial M}{\partial r} \right) + \frac{1}{r^{(D-1)}} M \frac{\partial M}{\partial r} \quad (89)$$

for the quantity

$$M(r, t) = \int_0^r \rho(r') S_D r'^{D-1} dr', \quad (90)$$

which represents the mass contained within the sphere of radius r . The appropriate boundary conditions are

$$M(0, t) = 0, \quad M(1, t) = 1. \quad (91)$$

It is also convenient to introduce the function $s(r, t) = M(r, t)/r^D$ satisfying

$$\frac{\partial s}{\partial t} = T \left(\frac{\partial^2 s}{\partial r^2} + \frac{D+1}{r} \frac{\partial s}{\partial r} \right) + \left(r \frac{\partial s}{\partial r} + Ds \right) s. \quad (92)$$

We look for self-similar solutions of the form

$$\rho(r, t) = \rho_0(t) f\left(\frac{r}{r_0(t)}\right), \quad r_0 = \left(\frac{T}{\rho_0}\right)^{1/2}. \quad (93)$$

In terms of the mass profile, we have

$$M(r,t) = M_0(t)g\left(\frac{r}{r_0(t)}\right) \quad \text{with} \quad M_0(t) = \rho_0 r_0^D, \quad (94)$$

and

$$g(x) = \int_0^x f(x') S_D x'^{D-1} dx'. \quad (95)$$

In terms of the function s , we have

$$s(r,t) = \rho_0(t)S\left(\frac{r}{r_0(t)}\right) \quad \text{with} \quad S(x) = \frac{g(x)}{x^D}. \quad (96)$$

Substituting the ansatz (96) into Eq. (92), we find that

$$\begin{aligned} \frac{d\rho_0}{dt}S(x) - \frac{\rho_0}{r_0} \frac{dr_0}{dt} x S'(x) = \rho_0^2 \left(S''(x) + \frac{D+1}{x} S'(x) \right. \\ \left. + x S(x) S'(x) + D S(x)^2 \right), \end{aligned} \quad (97)$$

where we have set $x = r/r_0$. The variables of position and time separate, provided that there exists α such that

$$\rho_0 r_0^\alpha = \kappa, \quad (98)$$

where κ is a constant. In that case, Eq. (97) reduces to

$$\begin{aligned} \frac{d\rho_0}{dt} \left(S(x) + \frac{1}{\alpha} x S'(x) \right) = \rho_0^2 \left(S''(x) + \frac{D+1}{x} S'(x) \right. \\ \left. + x S(x) S'(x) + D S(x)^2 \right). \end{aligned} \quad (99)$$

Assuming that such a scaling exists implies that $(1/\rho_0^2) \times (d\rho_0/dt)$ is a constant that we arbitrarily set equal to α (note that this convention is different from the one adopted in Ref. [1]). This leads to

$$\rho_0(t) = \frac{1}{\alpha} (t_{coll} - t)^{-1}, \quad (100)$$

so that the central density becomes infinite in a finite time t_{coll} . The scaling equation now reads

$$\alpha S + x S' = S'' + \frac{D+1}{x} S' + S(x S' + D S). \quad (101)$$

For $x \rightarrow +\infty$, we have asymptotically

$$S(x) \sim x^{-\alpha}, \quad g(x) \sim x^{D-\alpha}, \quad f(x) \sim x^{-\alpha}. \quad (102)$$

C. Canonical ensemble

In the canonical ensemble in which the temperature T is a constant, we have¹

$$\alpha = 2, \quad \kappa = T. \quad (103)$$

In that case, the scaling equation (101) can be solved analytically. Following a procedure similar to the one developed in Ref. [1], we find that

$$S(x) = \frac{4}{D-2+x^2}. \quad (104)$$

Then, Eqs. (96) and (95) yield

$$g(x) = \frac{4x^D}{D-2+x^2}, \quad f(x) = \frac{4(D-2)}{S_D} \frac{D+x^2}{(D-2+x^2)^2}. \quad (105)$$

According to Eqs. (93) and (100), the central density evolves with time like

$$\rho(0,t) = \rho_0(t) f(0) = \frac{2D}{(D-2)S_D} (t_{coll} - t)^{-1}. \quad (106)$$

According to Eqs. (93) and (94), the core radius and the core mass evolve like

$$r_0(t) = \sqrt{2T} (t_{coll} - t)^{1/2}, \quad M_0(t) = \frac{1}{2} (2T)^{D/2} (t_{coll} - t)^{D/2-1}. \quad (107)$$

Note that for $D > 2$, the core mass goes to zero at the collapse time. At $t = t_{coll}$, we get the singular profile

$$\rho(r, t = t_{coll}) = \frac{4T(D-2)}{S_D r^2}, \quad M(r, t = t_{coll}) = 4T r^{D-2}. \quad (108)$$

Therefore, at $t = t_{coll}$ the free energy is finite and the system has *not* created a Dirac peak contrary to what might have been expected from the discussion of Appendix B and Ref. [37]. In fact, we show in Appendix E that the collapse continues after t_{coll} and that the Dirac peak is formed in the *post-collapse* regime of our Brownian model.

D. Microcanonical ensemble

In the microcanonical ensemble, the exponent α is not determined by simple dimensional analysis. In Ref. [1], we found numerically that the scaling equation (101) has physical solutions only for $\alpha \leq \alpha_{max}$, with $\alpha_{max} \approx 2.21$ for $D = 3$. We also argued that the system will select the exponent α_{max} , since it leads to a maximum increase of entropy. In this section, we show that in the limit of large dimension D , we can explicitly understand the occurrence of such a α_{max} .

¹The case $T = 0$ is treated in Appendix E.

In addition, we will present the derivation of perturbative expansions for α_{\max} and the scaling function S , in powers of D^{-1} .

Equation (101) can be formally integrated as a first-order differential equation (writing $S'' = S' \times [S''/S']$), leading to an expression of $S(x)$ as a function of x , $S(x)$ itself, and $S''(x)/S'(x)$,

$$\left| \frac{\alpha}{DS(x)} - 1 \right| = \left| \frac{\alpha}{DS(0)} - 1 \right| \times \exp \left[\alpha \int_0^x \frac{y dy}{y^2(1-S(y)) - y \frac{S''(y)}{S'(y)} - (D+1)} \right]. \quad (109)$$

We now define x_0 , such that $S(x_0) = \alpha/D$. Since S should be analytic, the foregoing relation implies for $x \rightarrow x_0$,

$$\int_0^x \frac{\alpha y}{F(y)} dy \sim \ln|x - x_0|, \quad (110)$$

where $F(y)$ is the function that occurs in the denominator of the integral in Eq. (109). From Eq. (110), we must have $F(y) = \alpha x_0(y - x_0)$ for $y \rightarrow x_0$, which implies $F(x_0) = 0$ and $F'(x_0) = \alpha x_0$. These conditions can be rewritten explicitly as

$$x_0^2 \left(1 - \frac{\alpha}{D} \right) - x_0 \frac{S''(x_0)}{S'(x_0)} - (D+1) = 0, \quad (111)$$

$$(\alpha - 2)x_0 = - \frac{d}{dx} \left[x^2 S(x) + x \frac{S''(x)}{S'(x)} \right]_{x_0}. \quad (112)$$

This preparatory work now allows the introduction of a systematic expansion in large dimension D for the scaling function S , the scaling exponent α , and x_0 . In this limit, let us neglect the contribution of the terms that are not of order D in the right-hand side of Eq. (101). This actually amounts to taking $F(y) \approx y^2 - D$ in Eq. (109). Within this approximation, we find

$$\left| \frac{\alpha}{DS(x)} - 1 \right| = \left| \frac{\alpha}{DS(0)} - 1 \right| \left| \frac{x^2}{D} - 1 \right|^{\alpha/2}, \quad (113)$$

which is an analytic function only if $\alpha = 2$. This leads to $x_0 = \sqrt{D}$, and to the more explicit form for S ,

$$S(x) = \frac{S(0)}{1 + \left(\frac{DS(0)}{2} - 1 \right) \frac{x^2}{D}}. \quad (114)$$

$S(0)$ remains undetermined, and will be fixed by the next-order approximation. Indeed, we can iteratively solve the full scaling equation, Eq. (101), by reinserting the zeroth-order solution into Eq. (109), and eventually continue this process

with the new improved scaling function, and so forth. Thus, expressing the conditions of Eq. (111) and Eq. (112), and defining $z = DS(0)/2$ [which will be of order $O(1)$], we obtain

$$x_0^2 = D + \frac{4}{z} + O(D^{-1}) \text{ or } x_0 = \sqrt{D} \left(1 + \frac{2}{zD} + O(D^{-2}) \right), \quad (115)$$

and

$$\alpha - 2 = \frac{4}{D} \left[\frac{1}{z} - \frac{2}{z^2} \right] + O(D^{-2}). \quad (116)$$

Equation (116) provides a relation between the possible values for α and the associated value of $S(0) = 2z/D$. Note that the function of z in the right-hand side of Eq. (116) has a well defined maximum. Hence, up to order $O(D^{-1})$, we find that $\alpha \leq \alpha_{\max}$, with

$$\alpha_{\max} = 2 + \frac{1}{2}D^{-1} + O(D^{-2}), \quad (117)$$

which is associated to the value $z = 4 + O(D^{-1})$ or $S(0) = 8/D + O(D^{-2})$. As α is necessarily greater than 2 (as the temperature cannot vanish), a solution exists for any $\alpha \in [2, \alpha_{\max}]$. As already mentioned, α_{\max} is dynamically selected as it leads to the maximum divergence of the entropy and the temperature [see Eq. (127) below].

Inserting Eq. (114) into Eq. (109), we find the next-order approximation for S ,

$$\left| \frac{\alpha}{DS(x)} - 1 \right| = \left| \frac{\alpha}{DS(0)} - 1 \right| \left| \frac{x^2}{x_0^2} - 1 \right|^{(\alpha/2)(1-\phi)} \left[\frac{x^2}{x_1^2} + 1 \right]^{\alpha\phi/2}, \quad (118)$$

where x_0 is given by Eq. (115), and x_1 and ϕ are defined by

$$x_1^2 = \frac{D}{z-1} + \frac{2(z-2)}{z(z-1)} + O(D^{-1}),$$

$$\phi = \frac{2}{D} \left[\frac{1}{z} - \frac{2}{z^2} \right] + O(D^{-2}). \quad (119)$$

Again, the analyticity condition imposes that $\alpha/2(1-\phi) = 1$, which exactly leads to Eq. (116), and to the following explicit form for S :

$$S(x) = \frac{\alpha}{D} \left[1 + \left(1 - \frac{\alpha}{2z} \right) \left(\frac{x^2}{x_0^2} - 1 \right) \left(\frac{x^2}{x_1^2} + 1 \right)^{\alpha/2-1} \right]^{-1}. \quad (120)$$

This improved scaling function can be inserted again into the conditions expressed by Eqs. (111) and Eq. (112), leading to the next-order term in the expansion of α . After elementary, but cumbersome calculations, we end up with

$$\alpha - 2 = \frac{4}{D} \left[\frac{1}{z} - \frac{2}{z^2} \right] + \frac{8}{D^2} \left[\frac{5}{z} - \frac{26}{z^2} + \frac{31}{z^3} - \frac{6}{z^4} \right. \\ \left. - \left(\frac{1}{z} - \frac{7}{z^2} + \frac{14}{z^3} - \frac{8}{z^4} \right) \ln z \right] + O(D^{-3}). \quad (121)$$

This function has again a well defined maximum for

$$z \equiv \frac{D}{2} S(0) = 4 + \left(\frac{41}{2} - 6 \ln 2 \right) D^{-1} + O(D^{-2}), \quad (122)$$

associated to the value

$$\alpha_{\max} = 2 + \frac{1}{2} D^{-1} + \frac{11}{16} D^{-2} + O(D^{-3}). \quad (123)$$

This expansion gives $\alpha_{\max} = 2.24 \dots$ in $D=3$, in fair agreement with the exact value $\alpha_{\max} = 2.2097 \dots$ obtained numerically in Ref. [1]. In addition, the exponent $\alpha=2$ is associated to $z = 2 + 4D^{-1} + O(D^{-2})$. In principle, these expansions can be systematically pursued to the prize of increasingly complicated calculations.

Finally note that Eqs. (93) and (100) lead to the following exact asymptotic for the central density $\rho(0,t)$:

$$\rho(0,t) \sim K_D(\alpha) (t_{\text{coll}} - t)^{-1}, \quad K_D(\alpha) = \frac{2z(\alpha)}{\alpha S_D}, \quad (124)$$

where we have used $f(0) = DS(0)/S_D$ and the definition of z . The function $z(\alpha)$ is determined implicitly by Eq. (121), up to order $O(D^{-2})$. For the special cases $\alpha=2$ and $\alpha = \alpha_{\max}$, we, respectively, find

$$K_D(2) = 2S_D^{-1} [1 + 2D^{-1} + O(D^{-2})], \quad (125)$$

$$K_D(\alpha_{\max}) = 4S_D^{-1} \left[1 + \left(\frac{39}{8} - \frac{3}{2} \ln 2 \right) D^{-1} + O(D^{-2}) \right], \quad (126)$$

which shows that $K_D(\alpha_{\max})$ is substantially greater than $K_D(2)$ (twice bigger in the infinite D limit, the ratio being even bigger for finite D , as $\frac{39}{8} - \frac{3}{2} \ln 2 \approx 3.835 \dots > 2$). This substantial difference was noted in Ref. [1], in the case $D=3$. Finally, as expected in the microcanonical ensemble, the temperature diverges during the collapse as $T(t) \sim (t_{\text{coll}} - t)^{-\alpha_T}$ with $\alpha_T = 1 - 2/\alpha$; see Eqs. (93), (98), and (100). The strongest divergence is obtained for $\alpha = \alpha_{\max}$. According to Eq. (123), we have

$$\alpha_T = 2 - \frac{2}{\alpha_{\max}} = \frac{1}{4} D^{-1} + \frac{9}{32} D^{-2} + O(D^{-3}). \quad (127)$$

If we plug $D=3$ in Eq. (127), we find the estimate $\alpha_T \approx 0.11 \dots$ in fair agreement with the exponent measured numerically in [1], $\alpha_T \approx 0.1$. At $t = t_{\text{coll}}$, the entropy is infinite and the system has a ‘‘core-halo’’ structure (i.e., it is not a Dirac peak) with a vanishing mass in the core. This corresponds to a *small* number of particles packed together (or

just a binary) leading to an infinite density but a weak mass $M_c \ll M$. This structure is in agreement with the discussion of Appendix A and Ref. [37].

IV. THE TWO-DIMENSIONAL CASE

A. The critical temperature

In two dimensions, the dynamical equation (89) for the mass profile reads

$$\frac{\partial M}{\partial t} = 4Tu \frac{\partial^2 M}{\partial u^2} + 2M \frac{\partial M}{\partial u}, \quad (128)$$

after the change of variable $u = r^2$ has been effected. Looking for a stationary solution, and using $uM'' = (uM')' - M'$, Eq. (128) is readily integrated leading to

$$M(u) = \frac{4T}{4T-1} \frac{u}{1 + \frac{u}{4T-1}}. \quad (129)$$

Note that $M(1)=1$, which ensures that the whole mass is included in this solution. Using $\rho = M'/\pi$, we find that the density profile is given by

$$\rho(r) = \frac{4\rho_0}{\pi} \frac{1}{[1 + (r/r_0)^2]^2}, \quad (130)$$

with

$$r_0 = \sqrt{4T-1} \quad \text{and} \quad \rho_0 r_0^2 = T. \quad (131)$$

This solution exists provided that $T > T_c = 1/4$, which defines the collapse temperature. We have thus recovered the result (41) by a slightly different method. Note that the value of T_c and the dependence of r_0 and ρ_0 on the temperature coincide with the exact results obtained within the conformal field theory [38]. In the following, T is set constant (canonical description) as we have already seen that the gravothermal catastrophe does not exist in the microcanonical ensemble in two dimensions.

B. Scaling collapse for $T = T_c$

We now address the dynamics at the critical temperature $T = T_c = 1/4$. We note that contrary to what happens in other dimensions, the central density diverges at T_c . Thus, in analogy with critical phenomena, we anticipate a scaling solution for $M(u,t)$, of the form

$$M(u,t) \approx \frac{(a(t)+1)u}{1+a(t)u}, \quad (132)$$

which preserves the scaling form obtained above T_c , and which satisfies the boundary condition $M(1,t)=1$. The corresponding density profile is

$$\rho(r,t) = \frac{a(t)+1}{\pi} \frac{1}{(1+a(t)r^2)^2}. \quad (133)$$

The central density

$$\rho(0,t) = \frac{a(t)+1}{\pi}, \quad (134)$$

is expected to diverge for $t \rightarrow +\infty$, so that $a(t)$ is also expected to diverge.

Inserting the ansatz Eq. (132) into Eq. (128) shows that the left-hand term is indeed negligible compared to both terms of the right-hand side, to leading order in a . So far, this prevents us from determining a dynamical equation for a . In order to achieve that, we must solve Eq. (128) to the next order in a^{-1} . We thus look for a solution of the form

$$M(u,t) = \frac{a(t)u}{1+a(t)u} + a(t)^{-1}h(u,t), \quad (135)$$

where $h(u,t)$ is expected to be of order $O(1)$, and should satisfy $h(0,t)=0$ and $h(1,t)=1$ (the total integrated mass should be 0 and 1, respectively, for $u=0$ and $u=1$), and $\frac{\partial h}{\partial u}(0,t)=0$, which ensures that Eq. (134) is exactly obeyed, defining $a(t)$ without any ambiguity. The contribution of $\partial M/\partial t$ in the left-hand side of Eq. (128) is dominated by the time derivative of Eq. (132):

$$\frac{\partial}{\partial t} \left[\frac{(1+a(t))u}{1+a(t)u} \right] = \frac{u(1-u)}{(1+au)^2} \frac{da}{dt}, \quad (136)$$

which will be checked self-consistently hereafter. In addition, nonlinear terms in h in the right-hand side are also negligible. Therefore, h satisfies

$$\frac{au(1-u)}{(1+au)^2} \frac{da}{dt} = u \frac{\partial^2 h}{\partial u^2} + 2 \frac{\partial}{\partial u} \left(\frac{au}{1+au} h \right). \quad (137)$$

Actually, for a given time, this equation becomes an ordinary differential equation involving only one variable u , as a and da/dt appear as parameters. Equation (137) can be integrated leading to a first-order equation in h , which can be solved easily. Defining $v=au$, we finally get

$$h(u,t) = a^{-1} \left(1 + \frac{2}{a} \right) \frac{da}{dt} (1+v)^{-2} \left[(v^2-1) \ln(1+v) + v(1-2v) + 2v \int_0^v \frac{\ln(1+z)}{z} dz - \frac{2v^2+v^3}{2(a+2)} \right], \quad (138)$$

which depends on time only through the variables a and da/dt . Now, da/dt is determined by imposing the boundary condition $h(1,t)=1$, which leads to

$$\frac{da}{dt} = \frac{a}{\ln a - 5/2} [1 + O(\ln a^{-2})]. \quad (139)$$

One can solve iteratively Eq. (128), by adding the time derivative of the above solution to the left-hand side, in order to compute an improved h . To leading order, the form of Eq. (138) is preserved. However, new terms are generated which

are important for $v \sim a$ ($u \sim 1$), and which generate terms of order $O(a/\ln^3 a)$ in the expansion for da/dt . This explains the form of the error term in Eq. (139).

Integrating Eq. (139) for large time, we get the exact asymptotic expansion for large time

$$a(t) = \exp\left(\frac{5}{2} + \sqrt{2t}\right) [1 + O(t^{-1/2} \ln t)]. \quad (140)$$

For $t \rightarrow +\infty$, the central density diverges like $a(t)$ and the core radius goes to zero like $a(t)^{-1/2}$. In addition, the scaling solution (133) at $T=T_c$ goes to a Dirac peak containing the whole mass [see Eq. (42)], as the decay exponent of the scaling function is 4, which is strictly greater than 2.

C. Collapse for $T < T_c$

For $D=2$, the scaling equation associated to Eq. (89) does not display any physical solution when solved numerically. In this section, we thus present a special treatment adapted to this case. The principal difference with other dimensions is the divergence of the central density at T_c , and the occurrence of a scaling solution at this temperature.

Strictly below T_c , we expect a finite time collapse. Close to the center, the solution takes the form

$$M(u,t) \approx 4T \frac{a(t)u}{1+a(t)u}, \quad (141)$$

where again the left-hand side of Eq. (128) is negligible compared to each term on the right-hand side. We thus look for a solution of the type

$$M(u,t) = 4T \frac{a(t)u}{1+a(t)u} + h(u,t), \quad (142)$$

where h is of order $O(1)$ as it contains a finite fraction of the total mass, since the first term contains a mass of order $4T < 1$. Inserting this ansatz in the dynamical equation (128), we obtain

$$\frac{1}{4T} \frac{\partial h}{\partial t} + \frac{da}{dt} \frac{u}{(1+au)^2} = u \frac{\partial^2 h}{\partial u^2} + 2 \frac{\partial}{\partial u} \left(\frac{au}{1+au} h \right) + 2h \frac{\partial h}{\partial u}. \quad (143)$$

One can look for a scaling solution of the type

$$h(u,t) = a^{\gamma-1} H(au) \quad \text{with} \quad H(v) \sim cv^{1-\gamma} \quad \text{when} \quad v \rightarrow +\infty, \quad (144)$$

so that the mass included in this scaling profile $h(1,t)=c=O(1)$. With this definition, the density profile decays for large distance as $\rho \sim r^{-\alpha}$, with $\alpha=2\gamma$. Inserting this ansatz in Eq. (143), we obtain

$$\begin{aligned} & \left[\frac{1}{4T} (vH' + (\gamma-1)H) + a^{1-\gamma} \frac{v}{(1+v)^2} \right] \frac{da}{dt} a^{-2} \\ & = vH'' + 2 \left(\frac{v}{1+v} H \right)' + 2a^{\gamma-1} HH', \end{aligned} \quad (145)$$

where derivatives are with respect to the variable v . We are free to choose $a(t) = \pi\rho(0,t)/(4T)$, so that $H'(0) = H(0) = 0$. For small v , Eq. (145) leads to

$$\frac{da}{dt} = H''(0)a^{\gamma+1}. \quad (146)$$

Equation (145) has a global scaling solution only for $\gamma = 1$. However, we know that in this case the scaling equation obtained by setting $\gamma = 1$ does not display any physical solution. Thus, we conclude that there is no scaling solution obtained by imposing that all terms in Eq. (145) scale the same way. However, as we will see in the section devoted to numerical simulations, the direct simulation of Eq. (128) seems to display a scaling solution with $\gamma \approx 0.6-0.7$ for numerically accessible densities. Strictly speaking, this is totally excluded by the above equation, except if one allows γ to depend very slowly on the density or a . For a given a , we thus want to solve Eq. (145), where the boundary conditions will ultimately select the effective value of γ , and that of da/dt . More precisely, once we impose $H'(0) = H(0) = 0$, and the condition of Eq. (146), we end up with a shooting problem for $H''(0)$ and γ . For large a , and $v \ll a$, it is clear that the nonlinear term of the right-hand side of Eq. (145) becomes irrelevant, and we drop it from now on.

In order to understand the origin of this shooting problem, and to obtain an accurate estimate of γ , let us solve Eq. (145) in the limit of very large a , in the range $1 \ll v \ll a$. In this regime, Eq. (145) simplifies to the following equation

$$\left[\frac{1}{4T} (vH' + (\gamma - 1)H) + a^{1-\gamma}v^{-1} \right] \omega = vH'' + 2H', \quad (147)$$

where

$$\omega = \frac{da}{dt} a^{-2} = H''(0)a^{\gamma-1}. \quad (148)$$

Let us now multiply this equation by $v^{\gamma-2}$ and integrate the resulting equation. After elementary manipulations, we obtain

$$\begin{aligned} H' + \left[\frac{3-\gamma}{v} - \frac{\omega}{4T} \right] H \\ = -\frac{\omega c}{4T} v^{1-\gamma} - \frac{\omega a^{1-\gamma}}{2-\gamma} v^{-1} \\ + (2-\gamma)(3-\gamma)v^{1-\gamma} \int_v^{+\infty} w^{\gamma-3} H(w) dw, \end{aligned} \quad (149)$$

where $c \sim O(1)$, which has been defined in Eq. (144), appears here as an integration constant. Then, one can integrate this differential equation that leads to the following self-consistent relation for H :

$$H(v) = v^{\gamma-3} \exp\left(\frac{\omega v}{4T}\right) \int_v^{+\infty} w^{3-\gamma} \exp\left(-\frac{\omega w}{4T}\right) F(w) dw, \quad (150)$$

where F is defined as the opposite of the right-hand side of Eq. (149),

$$\begin{aligned} F(v) = \frac{\omega c}{4T} v^{1-\gamma} + \frac{\omega a^{1-\gamma}}{2-\gamma} v^{-1} \\ - (2-\gamma)(3-\gamma)v^{1-\gamma} \int_v^{+\infty} w^{\gamma-3} H(w) dw. \end{aligned} \quad (151)$$

Equation (147) implies that $H(v) \sim \ln v$, when $v \rightarrow 0$ [of course, this apparent divergence does not occur in the full dynamical equation (145)]. Considering the prefactor $v^{\gamma-3}$ in Eq. (150), this behavior can be obtained if and only if

$$\int_0^{+\infty} w^{3-\gamma} \exp\left(-\frac{\omega w}{4T}\right) F(w) dw = 0. \quad (152)$$

As ω is expected to go to zero for large a as $\gamma < 1$ [see Eq. (148)], the dominant contribution of the integral of the third term in the definition of F comes from the large w region, for which H can be replaced by its asymptotic form [see Eq. (144)]. Hence, defining $\Gamma(x) = \int_0^{+\infty} w^x \exp(-w) dw$ and $\varepsilon = 1 - \gamma$, and using Eq. (148), the condition expressed in Eq. (152) can be rewritten as

$$c = \frac{\Gamma(1+\varepsilon)}{\varepsilon(1+\varepsilon)^2 \Gamma(1+2\varepsilon)} H''(0) \left(\frac{H''(0)}{4T}\right)^\varepsilon a^{-\varepsilon^2}. \quad (153)$$

As c is of order $O(1)$, we find that $\varepsilon \rightarrow 0$ as $a \rightarrow +\infty$. More precisely, in this limit, ε is the solution of the following implicit equation:

$$\varepsilon = \sqrt{\frac{\ln(K/\varepsilon)}{\ln a}}, \quad (154)$$

where $K = H''(0)/c + O(\varepsilon)$. Finally, we obtain

$$\varepsilon = 1 - \gamma = \sqrt{\frac{\ln \ln a}{2 \ln a}} (1 + O([\ln \ln a]^{-1})). \quad (155)$$

In conclusion, although the solution is not, strictly speaking, a true scaling solution, the explicit dependence of γ on a is so weak that an apparent scaling should be seen with an effective γ almost constant for a wide range of values of a . Hence, the total density profile is the sum of the scaling profile obtained at T_c with a T/T_c weight (behaving as a Dirac peak of weight T/T_c , at $t = t_{coll}$) and of a pseudoscaling solution associated to an effective scaling exponent slowly converging to $\alpha = 2$.

Let us illustrate quantitatively the time dependence of $\alpha = 2\gamma$. For example, taking arbitrarily $K = 1$ (the dependence on K is weak and vanishes for large a), Eq. (154) and Eq. (155), respectively, lead to $\gamma(a = 10^3) = 0.624 \dots$ and

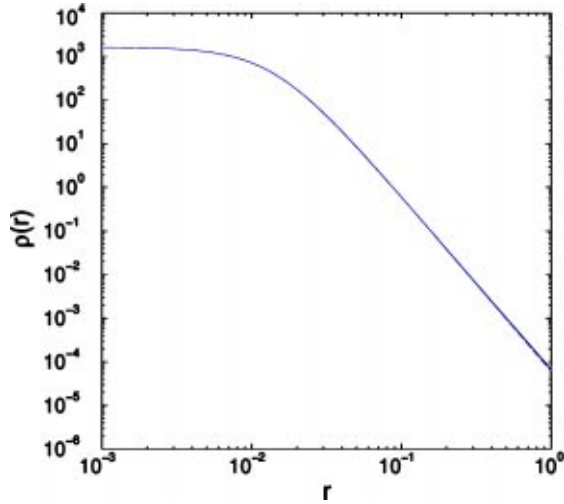


FIG. 10. At $T=T_c=1/4$, and when the central density has reached the value $\rho(0,t)\approx 1644.8\dots=[a(t)+1]/\pi$ [$a(t)\approx 5166.3\dots$], we have plotted the result of the numerical calculation compared to our exact scaling form $\rho(r,t)=[a(t)+1/\pi][1+a(t)r^2]^{-2}$ obtained in Eq. (133). The two curves are indistinguishable as the relative error is, as predicted, of order $a^{-1}\sim 10^{-4}$. Note finally that for this range of density, the density contrast is huge, of order 10^7 .

$\gamma(a=10^3)=0.626\dots$, and to $\gamma(a=10^5)=0.684\dots$ and $\gamma(a=10^5)=0.674\dots$ [note that the error between the asymptotic expansion of Eq. (155) and the implicit expression first grows before slowly decaying for $a\gg 10^{12}!$]. Finally, for the maximum value of a accessible numerically of order $a\sim 10^4$, we expect to observe an apparent scaling solution with $\gamma\approx 0.65$, or $\alpha=2\gamma\approx 1.3$.

D. Numerical simulations

In this section, we present direct numerical simulations of the Smoluchowski-Poisson system in 2D. Indeed, the three-dimensional case has been extensively studied in Ref. [1]. It has been shown that the scaling function as well as the corrections to scaling (which have been calculated for the canonical ensemble in Ref. [1]) are perfectly described by the theory. As the system behaves qualitatively the same for any dimension $D>2$, we have decided to focus on the numerical study of the $D=2$ case only, which displays some very rich behaviors, as exemplified in the present section.

We consider the system in the canonical ensemble, as the gravitational collapse does not occur in the microcanonical ensemble. In Fig. 10, we show the scaling function at T_c , as given by Eq. (133), finding a perfect agreement with the numerical simulation. In Fig. 11, we also display $a(da/dt)^{-1}$ as a function of $\ln a$, and find an asymptotic behavior fully compatible with that given by Eq. (139).

Below T_c , and in the accessible range of a (up to $a\sim 10^5$), we find an apparent scaling regime with $\alpha=2\gamma\approx 1.3$, as predicted in Sec. IV C. This is illustrated in Fig. 12, for $T=T_c/2=1/8$. Note that the effective γ or α can also be extracted from the time evolution of $a(t)$ or the central density [see Eq. (146)]. In Fig. 13, we show that this way of

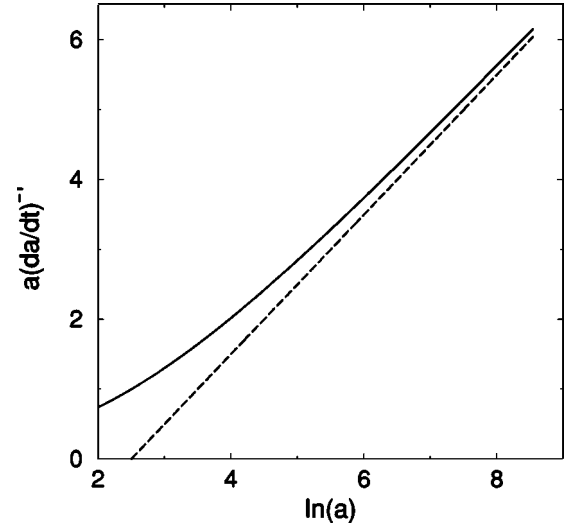


FIG. 11. We plot $a(da/dt)^{-1}$ as a function of $\ln a$, which is predicted to behave as $a(da/dt)^{-1}\sim \ln a - 5/2 + O([\ln a]^{-1})$ [see Eq. (139)]. Even for the moderate range of accessible densities ($a_{\max}\sim 5166$), we clearly find that the numerical result evolves toward the theoretical asymptotic (dashed line).

measuring γ is fully compatible with the value of the effective exponent $\alpha=2\gamma\approx 1.3$.

V. THE ONE-DIMENSIONAL CASE

When an equilibrium state exists, there is little hope to be able to solve the full Smoluchowski-Poisson system analytically in order to study the relaxation towards equilibrium. We shall consider a simpler problem in which a test particle

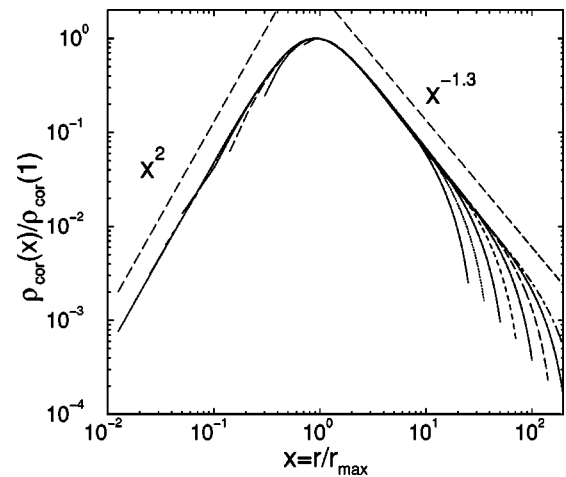


FIG. 12. At $T=T_c/2=1/8$, we have extracted the next correction to scaling $\rho_{\text{cor}}=\rho-4T\rho_{T=T_c}$, where $\rho_{T=T_c}$ is defined in Eq. (133). We have then plotted $\rho_{\text{cor}}(r,t)/\rho_{\text{cor}}(r_{\text{max}}(t),t)$ as a function of $x=r/r_{\text{max}}(t)$, where $r_{\text{max}}(t)$ is defined as the location of the maximum of $\rho_{\text{cor}}(r,t)$. Consistently with the apparent scaling observed, we found $r_{\text{max}}^{-1}(t)\sim\sqrt{a}\sim\sqrt{\rho_{\text{cor}}(r_{\text{max}}(t),t)}$. For $a=2^{n-1}\times 100$ ($n=1,\dots,8$), we have obtained a convincing data collapse associated to $\alpha=2\gamma\approx 1.3$, in agreement with the theoretical estimate of γ , in this range of a .

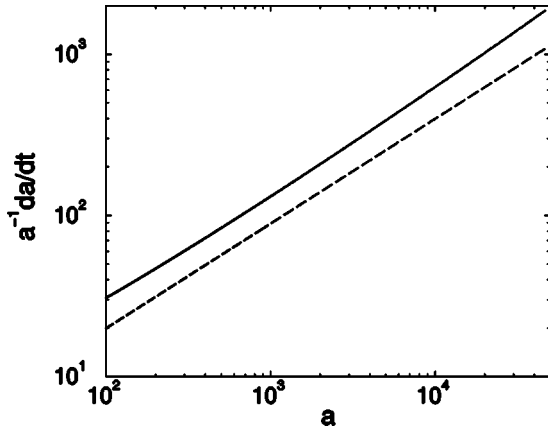


FIG. 13. We plot $a^{-1}(da/dt) \sim a^\gamma$ as a function of a , in order to extract the effective value of γ directly from the time evolution of the central density. We find that the effective γ is slowly growing with time, as predicted, and is of order $\gamma = \alpha/2 \approx 0.65$ (the dashed line has a slope equal to 0.65), which is fully compatible with the value extracted from Fig. 12, and the value expected from Eq. (154) in this range of a .

evolves in a medium of field particles at statistical equilibrium. The particles are assumed to create a *stationary* potential $\Phi_{eq}(\mathbf{r})$ that induces a drift of the test particle along the gradient of Φ_{eq} . In addition, the test particle is assumed to experience a diffusion process. If ρ denotes the density probability of finding the test particle in \mathbf{r} at time t , we expect the evolution of ρ to be determined by a Smoluchowski equation of the form

$$\frac{\partial \rho}{\partial t} = \nabla(T\nabla\rho + \rho\nabla\Phi_{eq}), \quad (156)$$

where $\Phi_{eq}(\mathbf{r})$ is the solution of the Boltzmann-Poisson equation (11). This means that we replace the true potential by its equilibrium value but still allow the density ρ to vary with time. As we shall see, it is possible to solve the Smoluchowski equation (156) analytically in $D=1$ by using an analogy with a problem of quantum mechanics. An equation of the form (156) has been proposed in Refs. [39,36] to model the motion of a test vortex in a bath of field vortices at statistical equilibrium. In that context, Eq. (156) can be derived from the N -body Liouville equation of the point vortex gas by using projection operator techniques.

It is well known that a Fokker-Planck equation such as Eq. (156) can be formally transformed into a Schrödinger equation with imaginary time. Indeed, performing the change of variable

$$\rho = \psi e^{-(1/2T)\Phi_{eq}}, \quad (157)$$

we find that the evolution of ψ is determined by an equation of the form

$$\frac{\partial \psi}{\partial t} = T\Delta\psi + \left(\frac{1}{2}\Delta\Phi_{eq} - \frac{1}{4T}(\nabla\Phi_{eq})^2 \right) \psi. \quad (158)$$

This can be written as a Schrödinger-type equation

$$\frac{\partial \psi}{\partial t} = T\Delta\psi - V(\mathbf{r})\psi, \quad (159)$$

with a potential $V(\mathbf{r}) = -\frac{1}{2}\Delta\Phi_{eq} + 1/4T(\nabla\Phi_{eq})^2$. So far, this transformation is general. If we now consider the one-dimensional case, the Boltzmann-Poisson equation (13) can be solved analytically and the potential $V(r)$ can be determined explicitly. Introducing the notations $\xi = \alpha r/\sqrt{2}R$ and $\tau = \alpha^2 T t/2R^2$ and using Eq. (24) we can rewrite Eq. (158) in the form

$$\frac{\partial \psi}{\partial \tau} = \Delta\psi + \left(\frac{2}{\cosh^2 \xi} - 1 \right) \psi. \quad (160)$$

A separation of the variables can be effected by the substitution

$$\psi(\xi, t) = \phi(\xi) e^{-\lambda t} \quad (\lambda \geq 0), \quad (161)$$

where ϕ is the solution of the ordinary differential equation

$$\frac{d^2 \phi}{d\xi^2} + 2 \left(E + \frac{1}{\cosh^2 \xi} \right) \phi = 0, \quad (162)$$

where we have set $\lambda - 1 = 2E$. The solutions of this Schrödinger equation are described in detail in Ref. [40]. The spectrum of positive energies is continuous. The spectrum of negative energies is discrete and reduces to $E_0 = -1/2$ (fundamental state). The first excited state in the continuum is $E_1 = 0$. We can check that the corresponding eigenfunctions are $\phi_0 = 1/\cosh \xi$ and $\phi_1 = \tanh \xi$. In order to obtain the qualitative behavior of the time dependent solution of Eq. (156), we neglect the contribution from the continuum states with $E > 0$, only keeping the $E = -1/2$ and $E = 0$ eigenstates.

Within this approximation and for sufficiently large times, we obtain

$$\psi(\xi, \tau) = \frac{A}{\cosh \xi} + B \tanh \xi e^{-\tau} \quad (\tau \rightarrow +\infty), \quad (163)$$

where A and B are constant. Returning to original variables, we get

$$\rho(r, t) = \rho_{eq}(r) \left\{ 1 + C \sinh \left(\frac{\alpha r}{\sqrt{2}R} \right) e^{-(\alpha^2 T/2R^2)t} + \dots \right\}, \quad (164)$$

where ρ_{eq} is given by Eq. (44) and $C = B/A$ is a constant. We find that the relaxation time is given by $t_{relax} = 2R^2/\alpha^2 T$.

VI. CONCLUSION

In this paper, we have studied the Boltzmann-Poisson equation and the Smoluchowski-Poisson system in various dimensions of space. Our study shows in particular how the nature of the problem changes as we pass from $D=3$ to $D=2$. We showed that the dimension $D=2$ is critical in the sense that the results obtained for $D > 2$ diverge if they are naively extrapolated to $D=2$. On a physical point of view,

the two-dimensional problem differs from the $D > 2$ case in two respects: in the 2D case, the central density of the equilibrium state is infinite at the critical temperature T_c while it is finite at T_c in higher dimensions. On the other hand, in $D = 2$, the self-similar collapse results in a Dirac peak that contains a finite fraction of mass, while for $D > 2$, the mass contained in the core tends to zero at the collapse time (but a Dirac peak is always formed in the canonical ensemble after t_{coll} as discussed in Appendix E). We have also evidenced another characteristic dimension $D = 10$ at which the nature of the problem changes. For $D \geq 10$ the classical spiral behavior of the caloric curve is lost. However, since the points on the spiral correspond to unstable states, which are therefore unphysical, this transition at $D = 10$ is not so critical and indeed the nature of the self-similar collapse does not show any transition at that dimension. It is interesting to note that the dependence of the phase diagram in the (E, T) and (u, v) planes with the dimension of space D shows some resemblance to the dependence of the phase diagram of confined polytropic spheres with the index n of the polytrope [41]. An extension of our study would be to relax the high friction limit and consider solutions of the Kramers-Poisson system and other relaxation equations described in Ref. [2]. These equations are expected to display qualitatively similar behaviors than those described here (i.e., gravitational collapse, finite time singularity, self-similar solutions, etc.), but their study appears to be of considerable difficulty since we now need to consider the evolution of the full distribution function in phase space instead of its lowest moments. We hope to come to that problem in future publications.

APPENDIX A: ABSENCE OF GLOBAL ENTROPY MAXIMUM IN THE MICROCANONICAL ENSEMBLE

In this appendix, we show the absence of global entropy maximum for a self-gravitating system in dimension $D > 2$. To that purpose, we shall construct a particular family of distribution functions which conserves mass and energy and which increases entropy indefinitely. As we shall see, it is necessary in the microcanonical ensemble to separate the system between a core and a halo. We describe the core and the halo by a distribution function of the form

$$f = \frac{1}{(2\pi T)^{D/2}} \rho e^{-v^2/2T}, \quad (\text{A1})$$

where the density ρ is assumed to be uniform in the core and the halo. We denote by ρ_c , M_c , R_c and ρ_h , M_h , R_h the density, mass, and radius of the core and the halo, respectively. We assume, by construction, that the temperature T is uniform throughout the system. With the distribution function (A1), we easily find that the kinetic energy and the entropy defined by Eqs. (3) and (5) can be written in each domain as

$$K = \frac{D}{2} MT, \quad (\text{A2})$$

$$S = \frac{D}{2} M \ln T - M \ln \rho. \quad (\text{A3})$$

Using Eq. (33) and the Gauss theorem (30), the potential energy of a spherically symmetric distribution of matter can be written as

$$W = -\frac{1}{D-2} \int_0^R \frac{GM(r)}{r^{D-2}} \frac{dM}{dr} dr, \quad (\text{A4})$$

for $D \neq 2$. From this expression, we can easily compute the potential energy of the core and the halo. Assuming $R_h \gg R_c$ (see below), we find that

$$W_c = -\frac{D}{D^2-4} \frac{GM_c^2}{R_c^{D-2}}, \quad W_h = -\frac{D}{2(D-2)} \frac{GM_c M_h}{R_h^{D-2}} - \frac{D}{D^2-4} \frac{GM_h^2}{R_h^{D-2}}. \quad (\text{A5})$$

The total energy of the system $E = E_c + E_h$ is therefore given by

$$E = \frac{D}{2} MT - \frac{D}{D^2-4} \frac{GM_c^2}{R_c^{D-2}} - \frac{D}{2(D-2)} \frac{GM_c M_h}{R_h^{D-2}} - \frac{D}{D^2-4} \frac{GM_h^2}{R_h^{D-2}}. \quad (\text{A6})$$

Let us first show the absence of global entropy maximum in an unbounded domain. In that case, Eq. (A6) determines the relation between the radius of the core and the radius of the halo (for fixed E , T , M_c and M_h). We have thus constructed a particular family of distribution functions parametrized by R_h that conserves the total mass and the total energy. We now take the limit $R_h \rightarrow +\infty$ that amounts to expanding the halo to infinity. Since the potential energy of the halo decreases, the potential energy of the core must increase so as to conserve energy. From Eq. (A6), we see that the radius of the core shrinks to a minimum radius R_c^{min} given by (we fix the temperature such that $E - (D/2)MT < 0$ by construction)

$$R_c^{min} = \left[\frac{-D}{D^2-4} \frac{GM_c^2}{E - \frac{D}{2}MT} \right]^{1/(D-2)}. \quad (\text{A7})$$

Therefore, the entropy of the core remains bounded whereas the entropy of the halo behaves like

$$S_h \sim -M_h \ln \left(\frac{M_h}{V_h} \right) \sim DM_h \ln R_h \rightarrow +\infty. \quad (\text{A8})$$

Therefore, for $D > 2$, an unbounded self-gravitating system can always increase entropy by taking a ‘‘core-halo’’ structure and by expanding the halo to infinity. To show heuristi-

cally that the separation between a core and a halo is necessary, let us consider the expansion of a uniform sphere with radius a . The equation

$$E = \frac{D}{2}MT - \frac{D}{D^2-4} \frac{GM^2}{a^{D-2}}, \quad (\text{A9})$$

determines the relation between the temperature and the radius of the configuration for a given mass and energy. When $a \rightarrow +\infty$, the relation (A9) becomes $E = (D/2)MT$ and can only be satisfied if $E > 0$. In that case, the entropy (A3) diverges like $S \sim DM \ln a \rightarrow +\infty$. However, for relevant situations in which $E < 0$, this argument cannot be used to prove the absence of global entropy maximum.

Let us now show the absence of global entropy maximum for a self-gravitating system confined within a box of radius R . We use the same distribution function as before with $R_h = R$. Equation (A6) now determines the relation between the temperature and the radius of the core (for fixed E , M_c , M_h , and R). We take the limit $R_c \rightarrow 0$ which amounts to shrinking the core. Since the potential energy of the core goes to $-\infty$, the temperature must increase to $+\infty$ in order to conserve the total energy. More precisely, using Eq. (A6), we have

$$T = \frac{2}{D^2-4} \frac{GM_c^2}{MR_c^{D-2}} \rightarrow +\infty. \quad (\text{A10})$$

The entropy behaves like

$$\begin{aligned} S &\sim \frac{D}{2}M \ln T - M_c \ln \left(\frac{M_c}{V_c} \right) \\ &\sim -\frac{D}{2}(D-2) \left(M_h - \frac{4-D}{D-2} M_c \right) \ln R_c. \end{aligned} \quad (\text{A11})$$

If $M_h > (4-D)/(D-2)M_c$, which can always be assumed by construction, the entropy diverges as the core shrinks, proving the absence of global entropy maximum. This simple argument shows the natural tendency (in a thermodynamical sense) of a self-gravitating system to develop a dense and hot ‘‘core’’ surrounded by a low-density ‘‘halo.’’ It has to be noted that the natural evolution in the microcanonical ensemble is *not* to create a Dirac peak with all the mass concentrated at $r=0$. Indeed, let us consider the collapse of a homogeneous sphere of mass M and radius a . If we fix the energy and let $a \rightarrow 0$, Eq. (A9) shows that the temperature behaves like

$$T = \frac{2}{D^2-4} \frac{GM}{a^{D-2}} \rightarrow +\infty. \quad (\text{A12})$$

On the other hand, according to Eq. (A3), the entropy behaves like

$$S \sim \frac{D}{2}M \ln T - M \ln \left(\frac{M}{V} \right) \sim -\frac{D}{2}(D-4)M \ln a. \quad (\text{A13})$$

If $D < 4$, the entropy goes to $-\infty$ as $a \rightarrow 0$. Therefore, the formation of a Dirac peak, which would lead to a *decrease* of entropy, is not favorable in the microcanonical ensemble. This is the case in particular for the usual dimension $D = 3$. Equation (A11) shows that the divergence of entropy requires that the mass contained in the halo is larger than the mass contained in the core. More precisely, the increase of entropy is maximum when only two particles (a binary) are tightly bound in the core while the rest of the particles are widespread in the halo (so that $M_c \ll M_h \sim M$). These results show that the ultimate fate of a self-gravitating system in the microcanonical ensemble is to form a tight binary surrounded by a diffuse halo. In this sense, there is no equilibrium state for a self-gravitating system, even in theory. However, as discussed in Refs. [37,42], this process can take a very long time so that the system may be found in practice in a *metastable* state corresponding to a local entropy maximum (see Sec. II). For $D > 4$, the formation of a Dirac peak leads to a divergence of entropy to $+\infty$ so that the core-halo structure is not necessary for entropy increase.

APPENDIX B: ABSENCE OF GLOBAL MAXIMUM OF FREE ENERGY IN THE CANONICAL ENSEMBLE

In this appendix, we show the absence of global maximum of free energy for a self-gravitating system in dimension $D > 2$ and for $T < T_c = GM/4$ in $D = 2$. Contrary to the microcanonical ensemble, we do *not* have to separate the system between a core and a halo. According to Eqs. (6), (9), and (A9), the free energy of a uniform sphere of mass M , radius a and temperature T (fixed) is

$$J = -M \ln \left(\frac{M}{V} \right) + \frac{D}{D^2-4} \frac{GM^2}{Ta^{D-2}}, \quad (\text{B1})$$

within an unimportant additional constant. For $a \rightarrow +\infty$, the free energy behaves like $J \sim DM \ln a$ and diverges. This proves the absence of global maximum of free energy for an unbounded self-gravitating system. If the system is now confined within a box of radius R , we consider the limit of Eq. (B1) for $a \rightarrow 0$ and find again that $J \rightarrow +\infty$ due to the divergence of the potential energy. This simple argument shows the natural tendency (in a thermodynamical sense) of a self-gravitating system to develop a Dirac peak in the canonical ensemble for any dimension $D > 2$. This contrasts with the microcanonical ensemble. The difference of behavior between microcanonical and canonical ensembles regarding the formation of a core-halo structure or a Dirac peak is another manifestation of ensemble inequivalence for self-gravitating systems.

In two dimensions, we consider a homogeneous disk of mass M and radius a at temperature T . It is easy to show that the total energy (8) of this disk is

$$E = MT + \frac{1}{2}GM^2(\ln a - 14), \quad (\text{B2})$$

with the convention $\Phi \sim GM \ln r$ at large distances. According to Eqs. (6), (9) and (B2), its free energy reads

$$J = M \ln T - M \ln \left(\frac{M}{\pi a^2} \right) - M - \frac{GM^2}{2T} \left(\ln a - \frac{1}{4} \right). \quad (\text{B3})$$

For $a \rightarrow 0$, the free energy behaves like

$$J \sim 2M \left(1 - \frac{GM}{4T} \right) \ln a. \quad (\text{B4})$$

Therefore, if $T < T_c = GM/4$ the free energy goes to $+\infty$ when we contract the system to a point. This is sufficient to prove the absence of global maximum of free energy below T_c : if sufficiently cold, the system has the tendency to create a Dirac peak. Note that for $T > T_c$, a true equilibrium state (global maximum of J) exists.

APPENDIX C: SOME USEFUL IDENTITIES

In this appendix, we establish the identities (76) and (77) that are needed in the stability analysis of Sec. II F. The first integral can be written after an integration by parts,

$$\begin{aligned} \int_0^\alpha \psi' \xi^D e^{-\psi} d\xi &= - \int_0^\alpha \xi^D \frac{d}{d\xi} (e^{-\psi}) d\xi \\ &= - \alpha^D e^{-\psi(\alpha)} + D \int_0^\alpha \xi^{D-1} e^{-\psi} d\xi. \end{aligned} \quad (\text{C1})$$

Using the Emden equation (13), we obtain

$$\int_0^\alpha \psi' \xi^D e^{-\psi} d\xi = - \alpha^D e^{-\psi(\alpha)} + D \alpha^{D-1} \psi'(\alpha). \quad (\text{C2})$$

Introducing the Milne variables (25), we get the identity (76). To establish the identity (77), we start from the relation

$$\begin{aligned} \int_0^\alpha \frac{\xi^{(1+D)/2} \psi'}{\xi} \frac{d}{d\xi} (\xi^{(1+D)/2} \psi') d\xi &= \alpha^D \psi'(\alpha)^2 \\ - \int_0^\alpha \frac{\xi^{(1+D)/2} \psi'}{\xi} \frac{d}{d\xi} (\xi^{(1+D)/2} \psi') d\xi \\ + \int_0^\alpha \xi^{D-1} (\psi')^2 d\xi, \end{aligned} \quad (\text{C3})$$

which results from a simple integration by parts. Therefore,

$$\begin{aligned} \int_0^\alpha \xi^{D-1} (\psi')^2 d\xi &= - \alpha^D \psi'(\alpha)^2 \\ + 2 \int_0^\alpha \xi^{(D-1)/2} \frac{d}{d\xi} (\xi^{(1+D)/2} \psi') \psi' d\xi, \end{aligned} \quad (\text{C4})$$

or, equivalently,

$$D \int_0^\alpha \xi^{D-1} (\psi')^2 d\xi = \alpha^D \psi'(\alpha)^2 - 2 \int_0^\alpha \xi^D \psi'' \psi' d\xi. \quad (\text{C5})$$

Using the Emden equation (13), we find that

$$(D-2) \int_0^\alpha \xi^{D-1} (\psi')^2 d\xi = - \alpha^D \psi'(\alpha)^2 + 2 \int_0^\alpha \xi^D \psi' e^{-\psi} d\xi. \quad (\text{C6})$$

Using Eq. (76) and introducing the Milne variables (25), we obtain the identity (77).

APPENDIX D: H-THEOREM AND VIRIAL THEOREM

To prove the H theorem for the Smoluchowski-Poisson system, we first take the time derivative of S given by Eq. (9), substitute explicitly for Eq. (79) and integrate by parts. This yields

$$\dot{S} = \frac{D}{2} M \frac{\dot{T}}{T} + \int \frac{1}{\xi \rho} (T \nabla \rho + \rho \nabla \Phi) \nabla \rho d^D \mathbf{r}. \quad (\text{D1})$$

The conservation of energy (8) in the microcanonical ensemble implies

$$\dot{E} = 0 = \frac{D}{2} M \dot{T} - \int \frac{1}{\xi} (T \nabla \rho + \rho \nabla \Phi) \nabla \Phi d^D \mathbf{r}, \quad (\text{D2})$$

where we have used Eq. (79) and integrated by parts. Eliminating \dot{T} between these two expressions, we obtain the H theorem (80). In the canonical situation in which T is constant, we take the time derivative of $J = S - (1/T)E$, substitute explicitly for Eq. (79), and integrate by parts. This yields

$$J = \int \frac{1}{T \rho \xi} (T \nabla \rho + \rho \nabla \Phi)^2 d^D \mathbf{r} \geq 0, \quad (\text{D3})$$

which is the form of the H -theorem in the canonical ensemble. S and J are the Lyapunov functionals of the Smoluchowski-Poisson system.

To establish the form of the virial theorem for the Smoluchowski-Poisson system, we first take the time derivative of the moment of inertia I defined by Eq. (83), substitute explicitly for Eq. (79) and integrate by parts. We get

$$\frac{dI}{dt} = - \int 2 \mathbf{r} \frac{1}{\xi} (T \nabla \rho + \rho \nabla \Phi) d^D \mathbf{r}. \quad (\text{D4})$$

Using the identity (33) and introducing the pressure $p = \rho T$, we obtain

$$\frac{1}{2} \xi \frac{dI}{dt} = - \int \mathbf{r} \cdot \nabla p d^D \mathbf{r} + (D-2)W, \quad (\text{D5})$$

or equivalently

$$\frac{1}{2} \xi \frac{dI}{dt} = - \int \nabla(p \mathbf{r}) d^D \mathbf{r} + \int p \nabla \cdot \mathbf{r} d^D \mathbf{r} + (D-2)W. \quad (\text{D6})$$

The first term in the rhs can be converted into a surface integral. Using furthermore $\nabla \cdot \mathbf{r} = D$, we find that

$$\frac{1}{2}\xi\frac{dI}{dt} = - \oint p\mathbf{r}\cdot d\mathbf{S}_D + D \int p d^D\mathbf{r} + (D-2)W. \quad (\text{D7})$$

Assuming that the pressure is constant on the surface (which is the case at least for a spherically symmetric distribution of matter in a spherical box) we can simplify the foregoing expression as

$$\frac{1}{2}\xi\frac{dI}{dt} = -p_b \oint \mathbf{r}\cdot d\mathbf{S}_D + 2K + (D-2)W, \quad (\text{D8})$$

where $K=(D/2)MT$ is the kinetic energy. Converting the first integral into a volume integral, using the divergence theorem, we finally establish Eq. (82).

APPENDIX E: THE CASE OF COLD SYSTEMS ($T=0$)

For $T=0$, Eq. (92) reduces to

$$\frac{\partial s}{\partial t} = \left(r \frac{\partial s}{\partial r} + Ds \right) s. \quad (\text{E1})$$

Looking for a self-similar solution of the form (96) and imposing the conditions (98) and (100), we find that the scaling profile satisfies

$$xS' + \alpha S = (xS' + DS)S. \quad (\text{E2})$$

Of course, for $T=0$, the exponent α cannot be determined on dimensional grounds, as the definition $r_0 = \sqrt{T/\rho_0}$ is not relevant anymore. As we will see, α will be determined by imposing that the scaling solution is analytic. Equation (E2) can be readily solved leading to the following implicit equation for S :

$$\left(\frac{\alpha}{D} - S(x) \right)^{1-\alpha/D} = Kx^\alpha S(x), \quad (\text{E3})$$

where K is an integration constant. Now, from the definition of S , we expect a small x expansion of the form $S(x) = S(0) + \frac{1}{2}S''(0)x^2 + O(x^4)$, which first implies that

$$S(0) = \frac{\alpha}{D}, \quad (\text{E4})$$

and that $(x^2)^{1-\alpha/D} \sim x^\alpha$, which finally leads to

$$\alpha = \frac{2D}{D+2} \quad \text{and} \quad K = \frac{D+2}{2} \left(\frac{1}{2} |S''(0)| \right)^{D/(D+2)}. \quad (\text{E5})$$

In terms of the scaling function $g(x)$ associated to the mass profile, Eq. (E3) can be rewritten as

$$g(x) = \frac{2x^D}{D+2} - \frac{|S''(0)|}{2} \left[\frac{D+2}{2} g(x) \right]^{(D+2)/D}, \quad (\text{E6})$$

where $S''(0) < 0$ is arbitrary. This leads to the exact large x asymptotic behavior

$$g(x) \sim \frac{2}{D+2} \left(\frac{4}{(D+2)|S''(0)|} \right)^{D/(D+2)} x^{D^2/(D+2)}. \quad (\text{E7})$$

Moreover, using $f(0) = DS(0)/S_D$ and Eq. (100) and (E4), we get the exact universal asymptotic behavior of the central density

$$\rho(0,t) \sim S_D^{-1} (t_{coll} - t)^{-1}. \quad (\text{E8})$$

Finally, we note that the implicit equation (E6) can be written as a parametric set of equations

$$g(y) = \frac{2}{D+2} y, \quad x(y) = \left[y + \frac{D+2}{4} |S''(0)| y^{(D+2)/D} \right]^{1/D}. \quad (\text{E9})$$

These results can be obtained by a different, more physical, method. We have indicated in Ref. [1] that, for $T=0$, the particles have a deterministic motion with equation

$$\frac{d\mathbf{r}}{dt} = \mathbf{u} = -\nabla\Phi. \quad (\text{E10})$$

For a spherically symmetric system, this can be rewritten as

$$\frac{dr}{dt} = -\frac{M(r,t)}{r^{D-1}}, \quad (\text{E11})$$

where $M(r,t)$ is the mass within r . If a denotes the initial position of the particle located at r at time t , we have

$$M(r,t) = M(a,0), \quad (\text{E12})$$

so Eq. (E11) can be integrated explicitly in

$$r^D = a^D - DM(a,0)t. \quad (\text{E13})$$

If $M(a,0)$ behaves like

$$M(a,0) = A(a^D - Ba^{D+2}) + \dots, \quad (\text{E14})$$

close to the origin (which is a regular expansion), then

$$M(r,t) = Aa^D(1 - Ba^2) \quad \text{with} \quad r^D = (1 - DAa^2t)a^D + DABa^{D+2}t. \quad (\text{E15})$$

Introducing the collapse time $t_{coll} = 1/DA$ and considering the limit $t \rightarrow t_{coll}$, we obtain

$$M(r,t) = \frac{a^D}{Dt_{coll}} \quad \text{with} \quad r^D = \frac{1}{t_{coll}} (t_{coll} - t)a^D + Ba^{D+2}. \quad (\text{E16})$$

Introducing the scaling variables

$$x = \frac{r}{(t_{coll} - t)^{(D+2)/2D}}, \quad y = \frac{1}{t_{coll}} \left[\frac{a}{(t_{coll} - t)^{1/2}} \right]^D, \quad (\text{E17})$$

we can put the solution in a parametric form

$$M(r,t) = \frac{1}{D}(t_{coll}-t)^{D/2}y \quad \text{with} \quad x = (y + Cy^{(D+2)/D})^{1/D}, \quad (\text{E18})$$

where C is a constant. At the collapse time $t = t_{coll}$,

$$\begin{aligned} M(r,t=t_{coll}) &= \frac{1}{DC^{D/(D+2)}}r^{D^2/(D+2)}, \quad \rho(r,t=t_{coll}) \\ &= \frac{D}{(D+2)S_D C^{D/(D+2)}}r^{-2D/(D+2)}. \end{aligned} \quad (\text{E19})$$

These results are of course equivalent to those obtained previously.

We can now use this method to study the evolution of the system for $t > t_{coll}$ (post-collapse solution). For $t = t_{coll} + \delta t$, according to Eqs. (E13) and (E19), the mass contained inside the sphere of radius $a_{coll} = C^{-1/2}\delta t^{(D+2)/2D}$ at $t = t_{coll}$ has collapsed at $r=0$, resulting in a Dirac peak of weight

$$M(0,t) = \frac{1}{DC^{D/2}}(t-t_{coll})^{D/2}. \quad (\text{E20})$$

Note that in a bounded domain the final collapse to a central Dirac peak containing the whole mass occurs in a finite time t_{end} after t_{coll} . For $r > 0$ (associated to $a > a_{coll}$), one has

$$M(r,t) = M(0,t) + \frac{1}{DC^{D/(D+2)}}(a^{D^2/(D+2)} - a_{coll}^{D^2/(D+2)}), \quad (\text{E21})$$

$$r^D = a^D \left[1 - \left(\frac{a_{coll}}{a} \right)^{2D/(D+2)} \right]. \quad (\text{E22})$$

Introducing the scaling variables

$$x = \frac{r}{a_{coll}}, \quad y = \left(\frac{a}{a_{coll}} \right)^{D^2/(D+2)} - 1 \quad (\text{E23})$$

we obtain the self-similar solution

$$M(r,t) = M(0,t)(1+y) \quad \text{with} \quad x = (1+y)^{D^2/(D+2)}[1 - (1+y)^{-2/D}]^{1/D}. \quad (\text{E24})$$

Subtracting the Dirac peak at $r=0$, and considering $x \ll 1$, for which $y \sim (D/2)x^D$, we find that the leading contribution to the mass profile for small r is

$$M(r,t) \approx \frac{r^D}{2\delta t}. \quad (\text{E25})$$

Hence the density profile does not diverge at $r=0^+$ for $t > t_{coll}$. Instead, the density approaches the constant value

$$\rho(0^+,t) = \frac{D}{2S_D\delta t}, \quad (\text{E26})$$

which decreases with time. The density profile is thus depleted on a scale $r \sim a_{coll} \sim \delta t^{(D+2)/2D}$, which increases with time. For $r \gg a_{coll}$, the density profile remains essentially unaffected.

In principle, the same phenomenon arises for any $0 < T < T_c$: the density profile obtained at t_{coll} ultimately collapses into a central Dirac peak at a time $t_{end} > t_{coll}$. This solves the apparent paradox that the solution at $t = t_{coll}$ has a vanishing central mass and a finite free energy. In fact, if we allow singular profiles to develop, the evolution continues for $t > t_{coll}$ and the Dirac peak with infinite free energy (predicted by statistical mechanics [23]) is formed during the post collapse regime of our Brownian model.² In practice, degeneracy effects (of quantum or dynamical origin) lead to a finite small core of finite density, controlled by the maximum allowed degeneracy [37].

²As discussed in Sec. II A, the results should be different in the microcanonical ensemble. We shall reserve the full description of the post-collapse regime for a future communication.

-
- [1] P.H. Chavanis, C. Rosier, and C. Sire, *Phys. Rev. E* **66**, 036105 (2002).
[2] P.H. Chavanis, J. Sommeria, and R. Robert, *Astrophys. J.* **471**, 385 (1996).
[3] T. Padmanabhan, *Phys. Rep.* **188**, 285 (1990).
[4] M.V. Penston, *Mon. Not. R. Astron. Soc.* **144**, 425 (1969).
[5] R.B. Larson, *Mon. Not. R. Astron. Soc.* **147**, 323 (1970).
[6] H. Cohn, *Astrophys. J.* **242**, 765 (1980).
[7] D. Lynden-Bell and P.P. Eggleton, *Mon. Not. R. Astron. Soc.* **191**, 483 (1980).
[8] J. Katz and D. Lynden-Bell, *Mon. Not. R. Astron. Soc.* **184**, 709 (1978).
[9] A.M. Polyakov, *Phys. Lett.* **103B**, 207 (1981).
[10] M.E. Cates, *Phys. Lett. B* **251**, 553 (1990).
[11] D. Carpentier and P. Le Doussal, *Phys. Rev. E* **63**, 026110 (2001).
[12] L. Onsager, *Nuovo Cimento, Suppl.* **6**, 279 (1949).
[13] J.D. Murray, *Mathematical Biology* (Springer, Berlin, 1991).
[14] C. Rosier, *C. R. Acad. Sci., Ser. I: Math.* **332**, 903 (2001).
[15] P. Biler and T. Nadzieja (unpublished).
[16] T. Padmanabhan, *Astrophys. J., Suppl. Ser.* **71**, 651 (1989).
[17] P.H. Chavanis, *Astron. Astrophys.* **381**, 340 (2002).
[18] G. Joyce and D. Montgomery, *J. Plasma Phys.* **10**, 107 (1973).
[19] J. Miller, *Phys. Rev. Lett.* **65**, 2137 (1990).
[20] R. Robert and J. Sommeria, *J. Fluid Mech.* **229**, 291 (1991).
[21] P.H. Chavanis and J. Sommeria, *J. Fluid Mech.* **314**, 267 (1996).
[22] P.H. Chavanis, in *Dynamics and Thermodynamics of Systems with Long Range Interactions*, Lecture Notes in Physics Vol. 602 edited by T. Dauxois, S. Ruffo, E. Arimondo, M. Wilkens,

- (Springer, Berlin, 2002).
- [23] M. Kiessling, *J. Stat. Phys.* **55**, 203 (1989).
- [24] J.J. Aly, *Phys. Rev. E* **49**, 3771 (1994).
- [25] V.A. Antonov, *Vestn. Leningr. Gos. Univ.* **7**, 135 (1962).
- [26] D. Lynden-Bell and R. Wood, *Mon. Not. R. Astron. Soc.* **138**, 495 (1968).
- [27] J. Katz, *Mon. Not. R. Astron. Soc.* **183**, 765 (1978).
- [28] S. Chandrasekhar, *An Introduction to the Theory of Stellar Structure* (Dover, New York, 1939).
- [29] E. Caglioti, P.L. Lions, C. Marchioro, and M. Pulvirenti, *Commun. Math. Phys.* **174**, 229 (1995).
- [30] G.L. Camm, *Mon. Not. R. Astron. Soc.* **110**, 305 (1950).
- [31] J. Binney and S. Tremaine, *Galactic Dynamics*, Princeton Series in Astrophysics (Princeton Univ. Press, Princeton, NJ, 1987).
- [32] J. Katz and M. Lecar, *Astrophys. Space Sci.* **68**, 495 (1980).
- [33] P.H. Chavanis, *Astron. Astrophys.* (to be published), e-print astro-ph/0207080.
- [34] H. Risken, *The Fokker-Planck Equation* (Springer, Berlin, 1989).
- [35] P.H. Chavanis, e-print cond-mat/0209096.
- [36] P.H. Chavanis, *Phys. Rev. E* **64**, 026309 (2001).
- [37] P.H. Chavanis, *Phys. Rev. E* **65**, 056123 (2002).
- [38] E. Abdalla and M.R. R Tabar, *Phys. Lett. B* **440**, 339 (1998).
- [39] P.H. Chavanis, *Phys. Rev. E* **58**, R1199 (1998).
- [40] L. Landau and E. Lifschitz, *Mécanique Quantique* (Editions MIR, Moscow, 1967).
- [41] P.H. Chavanis, *Astron. Astrophys.* **386**, 732 (2002).
- [42] P.H. Chavanis and I. Ispolatov, *Phys. Rev. E* **66**, 036109 (2002).